Parasitology International 83 (2021) 102358

Contents lists available at ScienceDirect

Parasitology International

journal homepage: www.elsevier.com/locate/parint

Plasmodium falciparum SURFIN$_{4.1}$ forms an intermediate complex with PTEX components and Pf113 during export to the red blood cell

Shinya Miyazaki [a,1], Ben-Yeddy Abel Chitama [a,b], Wataru Kagaya [a,c,2], Amuza Byaruhanga Lucky [a,b,3], Xiaotong Zhu [a,4], Kazuhide Yahata [a], Masayuki Morita [d], Eizo Takashima [d], Takafumi Tsuboi [d], Osamu Kaneko [a,b,*]

[a] Department of Protozoology, Institute of Tropical Medicine (NEKKEN), Nagasaki University, Nagasaki, Japan
[b] Program for Nurturing Global Leaders in Tropical and Emerging Infectious Diseases, Graduate School of Biomedical Sciences, Nagasaki University, Nagasaki, Japan
[c] Department of Environmental Parasitology, Graduate School of Tokyo Medical and Dental University, Tokyo, Japan
[d] Division of Malaria Research, Proteo-Science Center, Ehime University, Ehime, Japan

ARTICLE INFO

Dr D David Bzik

Keywords:
Malaria
Trafficking
Erythrocyte
Translocation
Protein complex

ABSTRACT

Plasmodium falciparum malaria parasites export several hundred proteins to the cytoplasm of infected red blood cells (RBCs) to modify the cell environment suitable for their growth. A *Plasmodium* translocon of exported proteins (PTEX) is necessary for both soluble and integral membrane proteins to cross the parasitophorous vacuole (PV) membrane surrounding the parasite inside the RBC. However, the molecular composition of the translocation complex for integral membrane proteins is not fully characterized, especially at the parasite plasma membrane. To examine the translocation complex, here we used mini-SURFIN$_{4.1}$, consisting of a short N-terminal region, a transmembrane region, and a cytoplasmic region of an exported integral membrane protein SURFIN$_{4.1}$. We found that mini-SURFIN$_{4.1}$ forms a translocation intermediate complex with core PTEX components, EXP2, HSP101, and PTEX150. We also found that several proteins are exposed to the PV space, including Pf113, an uncharacterized PTEX-associated protein. We determined that Pf113 localizes in dense granules at the merozoite stage and on the parasite periphery after RBC invasion. Using an inducible translocon-clogged mini-SURFIN$_{4.1}$, we found that a stable translocation intermediate complex forms at the parasite plasma membrane and contains EXP2 and a processed form of Pf113. These results suggest a potential role of Pf113 for the translocation step of mini-SURFIN$_{4.1}$, providing further insights into the translocation mechanisms for parasite integral membrane proteins.

1. Introduction

Malaria remains a public health concern in the tropical and sub-tropical regions of the world [1]. Among the causative protozoan pathogens of malaria, *Plasmodium falciparum* is responsible for the most severe form in humans and leads to high mortality of young children and pregnant women, especially in Sub-Saharan Africa. The emergence of *P. falciparum* resistance to artemisinin, the current front line anti-malarial drug, highlights the need to develop new anti-malarial drugs targeting essential biological steps of malaria parasites [2].

The pathologies associated with malaria are due to the *Plasmodium* parasite intraerythrocytic life cycle stage in which the parasite develops within and extensively modifies red blood cells (RBC). During this process *P. falciparum* exports several hundred parasite-encoded proteins to the RBC cytoplasm and surface [3]. The severity of *P. falciparum* is linked to RBC modification by malarial exported proteins; for example, parasite-encoded proteins by which the parasite-infected RBCs (iRBCs) gain a cytoadherence capacity for microvasculature endothelial cells [3]. Exported proteins by parasites are generally categorized into two types based on their sequence information. The first group possess a

* Corresponding author at: Department of Protozoology, Institute of Tropical Medicine (NEKKEN), Nagasaki University, Nagasaki, Japan.
E-mail address: okaneko@nagasaki-u.ac.jp (O. Kaneko).
[1] Department of Cellular Architecture Studies, Institute of Tropical Medicine (NEKKEN), Nagasaki university, Nagasaki, Japan
[2] Department of Parasitology and Research Center for Infectious Disease Sciences, Graduate School of Medicine, Osaka City University, Osaka 545-8585, Japan
[3] Department of Internal Medicine, Morsani College of Medicine, University of South Florida, 3720 Spectrum Boulevard, Suite 304, Tampa, FL 33612, United States
[4] Department of Immunology, College of Basic Medical Science, China Medical University, Shenyang, Liaoning 110122, People's Republic of China

https://doi.org/10.1016/j.parint.2021.102358
Received 19 March 2021; Received in revised form 8 April 2021; Accepted 14 April 2021
Available online 24 April 2021

pentameric amino acid motif RxLxE/Q/D, termed *Plasmodium* export element (PEXEL) or vacuolar targeting sequence (VTS) [4,5]. The second group lacks the PEXEL/VTS motif and is termed PEXEL negative exported proteins (PNEPs) [6,7]. Both groups of exported proteins are composed of many soluble and integral membrane proteins, which cooperatively work to support the nutrient uptake pathway, alter RBC rigidity, assign cytoadherence activity, and generate membranous structures within the iRBC such as Maurer's clefts [8–12]. This protein transport system is essential for parasite survival, and is therefore considered a potential drug target.

P. falciparum integral membrane proteins exported to the RBC surface play essential roles in parasite virulence mechanisms such as cytoadhesion, rosetting, and alteration of RBC rigidity [13]. Exported proteins include PfEMP1, RIFINs, STEVORs, and SURFINs, all encoded by multigene families in the *P. falciparum* genome [14–17]. PfEMP1 is exposed on the iRBC surface and its extracellular region binds to endothelial cells of blood vessels, resulting in severe outcomes such as cerebral malaria and placental malaria. Specific subtypes of RIFINs and STEVORs mediate binding to uninfected RBCs, leading to clumping termed rosetting [15,16]. A sub-type of SURFINs is additionally related to RBC rigidity, which is associated with malaria severity [10]. In an early step of trafficking these proteins are recruited to the parasite endoplasmic reticulum and Golgi network, then transferred to the parasite plasma membrane (PPM) by vesicular trafficking, where proteins are proposed to be exported by translocons in the PPM and parasitophorous vacuole membrane (PVM) to reach the RBC cytoplasm [6,18,19]. The PPM translocon was proposed based on the observation that the inhibition of the unfolding of REX2, an integral PNEP, resulted in the accumulation of this protein in the parasite cytoplasm [6]. The presence of a PPM translocon was also supported by a study showing that a transmembrane protein was unfolded before reaching to the PV space in *Plasmodium berghei* [20]. However, this hypothetical translocon remains to be identified.

A recent study described a translocation intermediate complex composed of an export-arrested protein and a pore component of the PVM translocon, termed *Plasmodium* translocon of exported proteins (PTEX) [21]. PTEX is a high molecular weight complex composed of three core proteins EXP2, HSP101, and PTEX150, and two accessory proteins PTEX88 and Trx2 [22–24]. A series of reverse genetic analyses revealed that the PTEX complex is essential for transport of many soluble and integral membrane proteins exported to the RBC in *P. falciparum* and the rodent malaria parasite *P. berghei* [25–28]. In this trafficking process the oligomeric EXP2 complex functions as a translocation pore for export substrates in the PVM [22,24,28–30]. Using an exported protein fused with a conditionally regulated unfoldable tag, Mesén-Ramírez et al. (2016) showed that the EXP2 pore complex was clogged with an export-arrested integral membrane protein, resulting in the formation of a translocation intermediate complex containing the exported protein and EXP2 [21]. PTEX components HSP101 and PTEX150 also interact with soluble PEXEL proteins [22,23,31]. An additional recent study has shown that PTEX components interact with an integral membrane protein PfEMP1 [32]. Based on these findings, PTEX is considered to translocate both soluble and integral membrane proteins. However, additional components in the translocation intermediate complex remain to be identified.

To characterize a translocation intermediate complex, we sought to isolate a membrane protein complex with SURFIN$_{4.1}$, an exported integral membrane protein for which we have dissected sequence requirements for trafficking to the RBC [33,34]. SURFINs are integral membrane PNEPs, encoded by 10 *surf* genes in the *P. falciparum* 3D7 line genome [17,35]. SURFIN$_{4.2}$ was originally identified as a protein trafficked to the parasite-iRBC surface via Maurer's clefts [17,36,37]. We have shown that SURFIN$_{4.1}$ is similarly transported across the PPM and PVM to Maurer's clefts, and this export is minimally determined by an N-terminal short sequence (N), transmembrane region (T), and a short cytoplasmic tail (C) [33]. The total length of the dissected SURFIN$_{4.1}$ region is 104 amino acids, which is comparable to the length of REX2, one of the smallest PNEPs (94 amino acids in length) [38]. Such a short sequence is useful to characterize the likely interactions with trafficking-related proteins, yet removing possible non-specific interactions meditated by other functional domains.

In this study, we identify a translocation intermediate complex with an exported integral membrane protein based on SURFIN$_{4.1}$ without using a conditionally regulated unfoldable tag. We used a transfectant expressing SURFIN$_{4.1}$N-T-C-TyGFP (mini-SURFIN$_{4.1}$), which is composed of minimal trafficking motifs identified in our previous study [33], a Ty1 peptide tag sequence, and green fluorescent protein (GFP). We applied immunoprecipitation, and mass spectrometric analyses using the transfectant expressing mini-SURFIN$_{4.1}$. We also performed proximity-dependent biotin identification (BioID) to identify proteins interacting with SURFIN$_{4.1}$. These approaches identified three core PTEX components EXP2, HSP101, PTEX150, plus a dozen uncharacterized or poorly characterized proteins including Pf113, which is released from merozoite dense granules and after invasion co-localizes with EXP2 on the parasite periphery. Our study provides insight into the protein translocation mechanism trafficking *P. falciparum* integral membrane proteins across the PPM by an unidentified translocon, and the PVM, which is driven by PTEX.

2. Experimental procedures

2.1. *P. falciparum* cultivation and transfection

P. falciparum MS822 was isolated in Thailand and maintained at Nagasaki University [39]. The 3D7 line was obtained from Dr. L. H. Miller [40], and the 3D7attB line was generated by Nkrumah et al. [41] and obtained through The Malaria Research and Reference Reagent Resource Center (MR4). Parasites were cultured essentially as described [42], in RPMI-1640 medium containing O+ RBCs at 2% hematocrit supplemented with 5% heat-inactivated pooled type AB+ human serum and 0.25% AlbuMAX I (Invitrogen), 200 μM hypoxanthine (Sigma), and 10 μg/mL gentamicin (Sigma). Human RBCs and plasma were obtained from the Nagasaki Red Cross Blood Center, Nagasaki, Japan.

P. falciparum transfection was performed by the spontaneous uptake method [43]. Plasmid DNA (100 μg) constructs were electroporated to uninfected RBCs in a 2 mm cuvette using the Gene Pulser Xcell Electroporation System (Bio-Rad). Transfected parasites were selected with 5 nM anti-folate drug WR99210 (a gift from D. Jacobus) or 1.25 μg/mL blasticidin-S from 4 days post-transfection. The WR99210 concentration was increased up to 20 nM during the maintenance.

2.2. Plasmid construction

To generate an expression vector for a BirA*-HA fusion protein, the BirA*-HA sequence was PCR-amplified using pcDNA$_{3.1}$MCS-BirA (R118G)-HA (Addgene) as a template DNA [44]. The amplified BirA*-HA region was introduced into the pCHD-CRT-5U-based expression vector by In-Fusion cloning (Takara, Japan). The pCHD-empty vector was firstly cloned by Gateway BP reaction and LR reaction using pB13, pENTR4/1_PfCRT5', and pCHDR-3/4 (gifts from G. McFadden; University of Melbourne, Australia) [45,46]. Then the BirA*-HA or SURFIN$_{4.1}$N-T-C-HA regions were inserted at a *Stu*I site by In-Fusion cloning. To make a construct for expression of SURFIN$_{4.1}$N-T-C-BirA*-HA, a new StuI site within the 5′ primer was used for introduction of the SURFIN$_{4.1}$N-T-C region.

To generate an expression vector for mini-SURFIN$_{4.1}$-mDHFR, the TyGFP coding region was firstly introduced into the *Sma*I site of the pB13 plasmid, then the SURFIN$_{4.1}$N-T-C region was PCR-amplified and introduced into the *Eco*RV site, resulting in the intermediate plasmid coding control mini-SURFIN$_{4.1}$ protein. Finally, the mDHFR coding region was PCR-amplified using pSEL1 (obtained from Addgene) as a template DNA, then introduced into the *Stu*I site. These pB13-based

intermediate plasmids coding mini-SURFIN$_{4.1}$-mDHFR or control protein were subjected to a Gateway Multisite LR recombination reaction with pENTR4/1_PfCRT5' and pLN-DEST-R43(II) containing a blasticidin-S deaminase (BSD) selectable marker [45]. TyGFP expression plasmids were constructed by introducing a TyGFP fragment into pB13 by the BP reaction and following LR reaction with pENTR4/1_PfCRT5' and pCHDR-3/4. The final expression plasmids were confirmed by diagnostic restriction enzyme digestion and nucleotide sequencing. Information of all oligonucleotide primers used in this study are shown in Table S3.

2.3. Solubilization of parasite proteins, chemical cross-linking, and immunoprecipitation

Ring and late trophozoite parasites-iRBCs were obtained by 60 h cultivation after sorbitol synchronization and were harvested by centrifugation. Parasite soluble protein and membrane proteins were prepared as described [33]. Parasite-iRBCs were treated with 0.15% (*w/v*) saponin and parasite pellets were suspended with PBS containing 1 mM EDTA and a proteinase inhibitor cocktail (PI; cOmplete, EDTA-free, Roche), then adjusted to a final concentration of 1×10^7 parasite/μL. After three cycles of freezing and thawing followed by centrifugation, supernatants were collected as freeze-thaw (F.T.) fractions containing soluble parasite proteins. The pellets were washed twice in PBS containing 1 mM EDTA and PI. The pellets were then resuspended in 1% Triton X-100 solubilization buffer (PBS containing 1 mM EDTA, 10% glycerol, and PI) and adjusted to 1×10^7 parasite/μL. Solubilization was performed on ice for 1 h. After centrifugation, the supernatants were collected as Triton X-100 solubilized fractions. Solubilized fractions were stored at −80 °C until use. Approximately 300 mL culture (~3×10^9 parasites) was used for purification of proteins interacting with mini-SURFIN$_{4.1}$. Ring and late trophozoite parasite-iRBCs were harvested by centrifugation. After saponin treatment and extraction of soluble protein described above, parasite pellets were resuspended in solubilization buffer (3×10^6 parasite/μL). A 1/10 volume of DSP (Sigma) dissolved in dimethyl sulfoxide (DMSO) was mixed with the parasite suspension. Parasites were incubated on ice for 15 min. Then, cross-linking with DSP was quenched by addition of 1 M Tris HCl (pH 7.5), and the Tris concentration was adjusted to 20 mM. After centrifugation, supernatants were removed.

Immunoprecipitation with DSP chemical cross-linking was performed using a protocol described for the isolation of a translocation complex in chloroplasts [47]. DSP-treated parasite pellets were solubilized with 2% SDS and 0.5% Triton X-100 in Tris-buffered saline (TBS)-based solubilization buffer containing 1 mM EDTA, 10% glycerol, and PI (final 1×10^7 parasite/μL) at room temperature for 30 min. After centrifugation, the supernatants were collected as an input fraction. To enable antibodies to interact with target antigens, solubilized fractions were 20-fold diluted with 0.5% Triton X-100 in TBS-based solubilization buffer. Diluted parasite proteins (5×10^8 parasites) were mixed with 2 μL of mouse monoclonal anti-Ty1 (2 μg/μL), rabbit polyclonal anti-EXP2, rabbit polyclonal anti-HSP101, rabbit polyclonal anti-PTEX150, or rabbit polyclonal Pf113, and incubated at room temperature for 2 h with gentle rotation. Solubilized fractions were then mixed with 20 μL of a 50% suspension of Gamma bind G plus Sepharose (Protein G beads; Amersham) at room temperature for 2 h with gentle rotation. The mixture was centrifuged and the supernatant was collected as an unbound fraction. Beads were washed four times with 0.5% Triton X-100 in TBS-based solubilization buffer. To elute mini-SURFIN$_{4.1}$ protein complexes, the beads were then mixed with Ty1 peptide (2.4 μg/μL) dissolved in 0.5% Triton X-100 in TBS-based solubilization buffer (final 1×10^8 parasite/μL). After incubation with gentle rotation at 4 °C for 12 h, the beads were centrifuged and the supernatants were collected as an immunoprecipitated fraction. Alternatively, the beads were boiled in SDS-PAGE loading buffer to elute bound proteins (final 1×10^8 parasite/μL).

2.4. Generation of Pf113 antibodies

To characterize Pf113 we generated a recombinant N-terminal GST tagged Pf113 using the wheat germ cell-free protein synthesis system (WGCFS) as described [48]. Briefly, a fragment encoding Pf113 (PF3D7_1420700: amino acid positions [aa] K_{97}–S_{948}) sequence, was PCR-amplified from cDNA obtained from schizont-rich *P. falciparum* 3D7 parasites using primers Pf113-sense and Pf113-antisense (Table S3). The amplified DNA fragment was cloned into the pEU-E01-GST-TEV-MCS-N2 plasmid (CellFree Sciences, Matsuyama, Japan) and GST-fused recombinant protein was expressed using WGCFS (CellFree Sciences). Expressed recombinant GST-Pf113 was then affinity purified using a glutathione-Sepharose 4B column (GE Healthcare, Camarillo, CA, USA). To generate Pf113 antisera, 250 μg or 20 μg of purified recombinant GST-Pf113 with Freund's complete adjuvant was used to subcutaneously immunize a Japanese white rabbit or intraperitoneally immunize two BALB/c female mice (Kitayama Labes, Ina, Japan), followed by two booster immunizations of 250 μg in rabbit or 20 μg in mouse of GST-Pf113 with Freund's incomplete adjuvant at 3-week intervals. Antisera was collected 14 days after the last immunization. The animal work was conducted by Kitayama Labes (Ina, Japan) in compliance with the guidelines based on "Charter for Laboratory Animal Welfare" (Japanese Society for Laboratory Animal Resources).

2.5. SDS-PAGE and Western blotting

Parasite protein fractions were subjected to electrophoresis on 5–20% polyacrylamide gradient mini gels (ATTO, Japan) under reducing or non-reducing conditions, then transferred to PVDF membranes (Millipore). The membranes were probed with mouse anti-Ty1 monoclonal antibody (1:500, Diagenode), rat anti-HA monoclonal antibody (1:1000, 3F10 Roche), rabbit anti-EXP2 polyclonal antibody (1:5000), rabbit anti-HSP101 polyclonal antibody (1:1000), rabbit anti-PTEX150 antibody (1:1000), or mouse or rabbit anti-Pf113 polyclonal antibodies (1:1000) for 1 h at room temperature. Rabbit polyclonal antisera against EXP2 (D_{25} to E_{287}; PF3D7_1471100), HSP101 (A_{27}-P_{809}; PF3D7_1116800), and PTEX150 (E_{130}-N_{993}; PF3D7_1436300) were generated as described above (Generation of Pf113 antibodies). The membranes were then incubated with horseradish peroxidase (HRP)-conjugated goat anti-mouse, anti-rabbit, or anti-rat antibodies (Promega) at a concentration of 1:25,000. Bands were visualized with Immobilon Western Chemiluminescent HRP substrate (Millipore) or ECL Select Western Blotting Detection Reagent (GE Healthcare) and detected using a chemiluminescence detection system (LAS-4000EPUVmini; Fujifilm). The relative molecular sizes of the proteins were measured based on a molecular size standard (Precision plus Dual colour standards; Bio-Rad).

2.6. Blue native PAGE (BN-PAGE)

BN-PAGE was performed using the NativePAGE™ Novex® Bis-Tris Gel system (Invitrogen) according to the manufacturer's protocol. Protein samples were mixed with loading buffer containing 0.25% Coomassie Brilliant Blue (CBB) G-250 and 1% Triton X-100. Solubilized fractions were subjected to electrophoresis at 4 °C with 120 V for 2 h. After electrophoresis, proteins were denatured by incubating the gels in SDS-PAGE electrophoresis buffer for 10 min, transferred to PVDF membranes using a Mini Trans-Blot® Cell (Bio-Rad) with 25 V at 4 °C for 12 h, then processed for immunoblot analysis.

2.7. Mass spectrometric analysis

Mass spectrometric analysis of immunoprecipitated proteins was performed as described [49]. The protein samples were briefly electrophoresed to introduce them into a gel and the bands (containing whole mixture of protein) were excised. The gel pieces were fixed with an

acetic acid/methanol solution, followed by fixation with 50% methanol. The gel pieces were then washed with distilled water and stored at −30 °C. LC-MS/MS analysis was performed at the W. M. Keck Biomedical Mass Spectrometry Laboratory, University of Virginia, USA according to their standard LC-MS/MS protocol. The data were analyzed using the SEQUEST search algorithm against a *P. falciparum* predicted protein database. The quantitative value (QV) is a normalized value with the sum of the unweighted spectrum counts for each sample and represents a relative quantity of each protein in the sample. Candidate interacting proteins were determined by the following criteria: proteins that showed QV ≧ 1 in the test sample and QV = 0 in the control sample, or QV in the test sample at least two-fold higher than control QV.

2.8. Proximity dependent biotinylation (BioID)

Approximately 200–300 mL of parasite-iRBC cultures were used for purification of biotinylated proteins. After sorbitol synchronization, transfectants expressing BirA*-fused proteins were cultured in the presence of 150 μM biotin (Wako, Japan) for 20 h. BirA* is a mutated biotin ligase from *E. coli*. Parasite-iRBCs were treated with 0.15% (*w/v*) saponin. Then parasite pellets were solubilized with 2% SDS and 0.5% Triton X-100 in TBS-based solubilization buffer. Solubilized fractions were diluted 20-fold with 0.5% Triton X-100 in TBS-based solubilization buffer. Diluted parasite proteins were subjected to affinity purification. One mL of solubilized fractions (2×10^8 parasites) were mixed with Dynabeads (MyOne streptavidin C1; Invitrogen), and incubated at room temperature for 4 h with gentle rotation. Dynabeads were washed four times with 0.1% SDS and 0.5% Triton X-100 in TBS-based solubilization buffer and the biotinylated proteins were eluted by boiling in 0.1% SDS and 0.5% Triton X-100 in TBS-based solubilization buffer (final 1×10^8 parasite/μL). Eluate fractions were applied to LC-MS/MS and Western blotting with HRP-conjugated streptavidin (1:40,000, Invitrogen).

2.9. Indirect immunofluorescence assay (IFA) and live imaging

IFA was performed basically as described [33]. Thin smears of mixed stages of parasite-iRBCs on glass slides were dried and fixed with 4% paraformaldehyde/0.075% glutaraldehyde (PFA) or acetone at room temperature, followed by blocking with 50 mM glycine in PBS for PFA fixation or Image-iT ™ FX Signal Enhancer (Molecular Probes) for acetone fixation. Smears were probed with anti-Ty1 (mouse monoclonal, 1:500), anti-HA (rat monoclonal 3F10, 1:100), anti-Pf113 (mouse polyclonal, 1:500), anti-SBP1 (rabbit polyclonal, 1:500), anti-EXP2 (rabbit polyclonal 1:500), anti-HSP101 (rabbit polyclonal, 1:1000), or anti-PTEX150 (rabbit polyclonal, 1:1000). Rabbit polyclonal antisera against SBP1 (Q_{258} to T_{337}; PF3D7_0501300) was generated as described above (Generation of Pf113 antibodies). Nuclei were stained with 4′,6-diamidino-2-phenylindole (DAPI, 1:500). Blood smears were then incubated with either Alexa-Fluor 488 goat anti-mouse antibody, Alexa-Fluor 594 goat anti-rabbit antibody, Alexa-Fluor 568 goat anti-rabbit antibody, and/or DyLight™ 488 goat anti-rat IgG antibody. For live imaging, parasite-iRBCs stained with Hoechst were spotted onto glass slides and cover slip. IFA and GFP fluorescence images were captured with a fluorescence microscope (LSM780; Carl Zeiss MicroImaging, Thornwood, NY) and processed on a Zeiss Axio Observer Z2 using Axiovision software. IFA smears were also observed by super resolution structured illumination (SR-SIM) imaging (LSM780/ERYRA PS1) using a 100× N.A. 1.46 alpha Plan-Apochromat oil-immersion objective (Zeiss), Diode laser, and EM-CCD camera iXon DU885 (Andor, UK) with 1900 × 1900 pixels. Filter sets used were DAPI (excitation / emission = 405 / BP420–480 nm), Alexa Fluor 488 (488 / BP495–560 nm), Alexa Fluor 568 (561 / BP570–640 nm). SR-SIM images were processed using ZEN software (Zeiss).

For co-localization of Pf113 and secretion organelles, IFA was performed as follows. Infected blood smears were fixed on glass slides with 4% paraformaldehyde at RT for 10 min, permeabilized with PBS-T (PBS containing 0.1% Triton X-100) at room temperature for 15 min, and blocked with PBS containing 5% nonfat milk (blocking solution) at 37 °C for 30 min. The slides were then incubated with rabbit anti-Pf113 antibodies (1:500) and co-stained at 37 °C for 1 h with mouse anti-AMA1 (PF3D7_1133400) antibody (1:100) as a microneme marker [48], mouse anti-RAP1 (PF3D7_1410400) antibody (1:1000) as a rhoptry body marker [50], mouse anti-RON2 (PF3D7_1452000) antibody (1:100) as a rhoptry neck marker [51], or mouse anti-RESA (PF3D7_0102200) mAb (1:200) as a dense granule marker [51]; followed by incubation at 37 °C for 30 min with Alexa Fluor 488-conjugated goat anti-rabbit IgG (Invitrogen, Carlsbad, CA) and Alexa Fluor 546-conjugated goat anti-mouse IgG (Invitrogen) as secondary antibodies (1:500). Nuclei were stained with DAPI (2 μg/mL) mixed with a secondary antibody solution. The slides were mounted in ProLong Gold Antifade reagent (Invitrogen) and observed using a confocal scanning laser microscope (LSM710; Carl Zeiss MicroImaging).

3. Results

3.1. Mass spectrometric analysis of mini-SURFIN$_{4.1}$ protein complexes identified potential interacting proteins including PTEX components and exported proteins

In this study we sought to identify the components of a malaria parasite protein export translocation intermediate using multiple biochemical approaches and utilizing a probe, mini-SURFIN$_{4.1}$. We previously established a *P. falciparum* transfectant line expressing mini-SURFIN$_{4.1}$ and showed that mini-SURFIN$_{4.1}$ was translocated to the RBC cytoplasm and reached Maurer's clefts (Fig. 1A, Fig.S1) [33]. To stabilize transient protein-protein interactions with mini-SURFIN$_{4.1}$, we used dithiobis(succinimidyl propionate) (DSP), a cell-permeable thiol-cleavable chemical cross-linker, which has been validated for stabilization of the PTEX complex [22,23]. We performed Blue Native polyacrylamide gel electrophoresis (BN-PAGE) using Triton X-100-solubilized fractions followed by Western blotting with anti-Ty1. Without DSP treatment, we observed an ~200-kDa mini-SURFIN$_{4.1}$ protein complex (Fig. S2A). DSP cross-linking (2 mM) promoted formation of high molecular weight protein complexes (Fig. S2A). The presence of smear bands suggests that a mixture of protein complexes contain mini-SURFIN$_{4.1}$. DSP chemical cross-linking was dose-dependent as shown by non-reducing SDS-PAGE (Fig. S2B). Because 1 mM DSP treatment was saturating (Fig. S2B), we selected this DSP concentration for further experiments.

Next, we performed immunoprecipitation to purify cross-linked mini-SURFIN$_{4.1}$ high molecular weight protein complexes. In our previous study, we observed that SURFIN$_{4.1}$ was not completely solubilized with Triton X-100 [33]. Thus, for immunoprecipitation experiments we solubilized parasite membrane fractions by a combination of sodium dodecyl sulfate (SDS) and Triton X-100. Electrophoresis analysis confirmed that mini-SURFIN$_{4.1}$ protein complexes were cross-linked (Fig. 1B, input lane) and that mini-SURFIN$_{4.1}$ protein complexes were efficiently purified by immunoprecipitation (Fig. 1B, IP lane). SDS-PAGE followed by ruby staining of these immunoprecipitated fractions revealed bands with sizes greater than 50 kDa, unique to the immunoprecipitated fraction from transfectants with cross-linking (Fig. 1C).

To identify components of mini-SURFIN$_{4.1}$ protein complexes, we used whole mixtures of immunoprecipitated fractions of transfectant and parent lines for liquid chromatography coupled with tandem mass spectrometry (LC-MS/MS) analysis. Mass spectrometry identified 71 parasite proteins (Table S1). We excluded 29 proteins for which no signal peptide sequence and transmembrane regions were predicted and 12 proteins which were localized in the parasite cytoplasm, such as within the endoplasmic reticulum, food vacuole, and mitochondrion. The remaining 30 proteins included three core components of the PTEX complex [22], EXP2, HSP101, and PTEX150; and two PTEX-associated proteins, parasitophorous vacuole protein 1 (PV1) and Pf113 [52] (Table 1). Two accessory PTEX components, PTEX88 and Trx2, were not

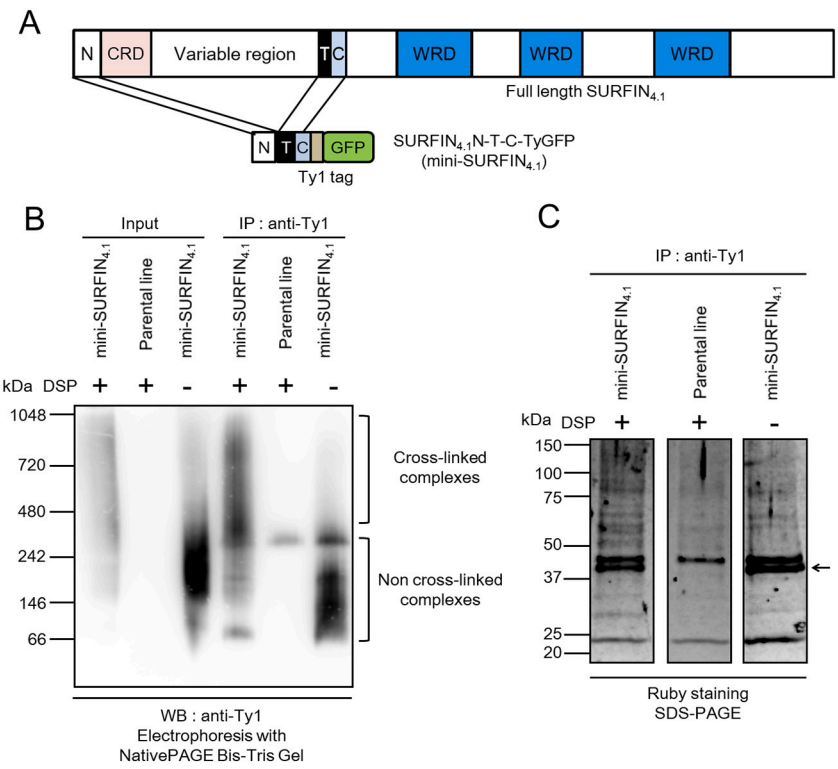

Fig. 1. Purification and proteomic analysis of cross-linked mini-SURFIN$_{4.1}$ protein complexes. (A) Schematic representations of endogenous SURFIN$_{4.1}$ and the mini-SURFIN$_{4.1}$ protein expressed in the transfectant line. Endogenous SURFIN$_{4.1}$ shown contains a cysteine-rich domain (CRD), variable region, and three tryptophan-rich domains (WRD). The mini-SURFIN$_{4.1}$ consists of an N-terminal short sequence (N, 50 amino acids), a transmembrane region (T, 24 amino acids), and a short cytoplasmic tail (C, 24 amino acids) followed by a Ty1 tag used for affinity purification. (B) Detection of the DSP cross-linked mini-SURFIN$_{4.1}$ protein complex in the solubilized and immunoprecipitated fractions. Parasite proteins from the transfectant and the parental parasite line were solubilized and then immunoprecipitated (IP) with anti-Ty1. Input fractions (1×10^8 parasites) and IP fractions (3×10^8 parasites) were subjected to NativePAGE Bis-Tris gel electrophoresis followed by Western blotting with anti-Ty1. Smeared bands were mainly detected above 242 kDa from the DSP-treated transfectant sample or below 242 kDa from the DSP-untreated transfectant sample. (C) Detection of potential interacting proteins by SDS-PAGE and ruby staining. The same IP fractions shown in panel B were applied to this experiment. The band with the arrow indicates mini-SURFIN$_{4.1}$ whose expected size is 44.5 kDa. Protein samples from the DSP-treated transfectant (mini-SURFIN$_{4.1}$, DSP+) and the parental line (DSP+) were subjected to mass spectrometric analysis.

identified by our mass spectrometric analysis (Table S1). Our proteomic analysis further identified seven PVM-residing proteins, EXP1, EXP3, ETRAMP4, 5, 10.1, 10.2, and Pfs16; and two PPM-residing proteins, PfATP4 and NCR1 (Table 1). Seven proteins exported to the iRBC cytoplasm were found, including SBP1, REX1, GBP130, PTP1, SEMP1, PEXEL-negative exported protein (PF3D7_0830400), and *Plasmodium* exported protein with unknown function (PF3D7_0301700), which might associate with mini-SURFIN$_{4.1}$ in the iRBC cytoplasm after translocation (Table 1). In addition, we identified the rhoptry body proteins RhopH2 and RhopH3, which were proposed to be translocated via the PTEX translocon [53]; and rhoptry neck protein 3 (RON3), which is essential for PTEX function (Table 1) [54]. The remaining six proteins included MFR4, MFR5, a putative thioredoxin-related protein, and three conserved *Plasmodium* proteins with unknown function (PF3D7_0811600, PF3D7_0721100, and PF3D7_0706100).

We performed a second LC-MS/MS analysis using parasite samples prepared independently. This analysis identified HSP101, EXP2, PV1, ETRAMP10.2, Pf113, and two exported proteins REX1 and GBP130 (Table 1, Experiment 2); however, PTEX150 was not detected. This analysis confirmed the reproducible interaction of the mini-SURFIN$_{4.1}$ with PTEX components and other proteins known to localize at the PV or exported to the iRBC cytoplasm, such as Pf113, PV1, ETRAMP10.2, REX1, and GBP130. MFR4 and MFR5 were also detected in this second experiment. Disruption of the gene loci encoding MFR4 or MFR5 orthologs in *P. berghei* revealed their roles in the mosquito stage or both blood and mosquito stages, respectively; however, their localization has not been determined [66].

3.2. BioID analysis of the SURFIN$_{4.1}$N-T-C region also identified PTEX components and a different set of interacting proteins

To cover a broader range of interactions with the SURFIN$_{4.1}$N-T-C region, we applied proximity dependent biotinylation identification (BioID) [44]. We generated a transfectant expressing the SURFIN$_{4.1}$N-T-C region fused with BirA*, a mutated biotin ligase from *Escherichia coli*, and a hemagglutinin (HA) tag (SURFIN$_{4.1}$N-T-C-BirA*-HA); as well as two control transfectants expressing the SURFIN$_{4.1}$N-T-C region fused with only an HA tag (SURFIN$_{4.1}$N-T-C-HA) and BirA* fused with an HA tag (BirA*-HA) (Fig. 2A). Protein expression of each transfectant was confirmed by Western blotting (Fig. 2B). IFA confirmed that SURFIN$_{4.1}$N-T-C-BirA*-HA co-localized with the Maurer's cleft marker SBP1 in addition to the parasite cytoplasmic signal (Fig. S3), whereas BirA*-HA localized within the parasite (Fig. S3). These results indicate that SURFIN$_{4.1}$N-T-C-BirA*-HA was translocated across the PPM and PVM and was correctly exported to Maurer's clefts.

Next, we assessed the biotinylation of parasite proteins using the SURFIN$_{4.1}$N-T-C-BirA*-HA. In the absence of biotin, a smeared band was detected by Western blotting with streptavidin-HRP only for the control BirA*-HA (Fig. 2C). In contrast, in the presence of biotin, smeared bands were detected in the lane for transfectants expressing SURFIN$_{4.1}$N-T-C-BirA*-HA or control BirA*-HA, but not in two control lanes expressing no BirA* (Fig. 2C). This suggests that exogenous biotin promotes the biotinylation of parasite proteins in a BirA* dependent manner. To identify the parasite proteins biotinylated by SURFIN$_{4.1}$N-T-C-BirA*-HA, we affinity-purified biotinylated proteins with streptavidin beads from the eluate fractions of SURFIN$_{4.1}$N-T-C-BirA*-HA and BirA*-HA (Fig. 2D) and subjected them to LC-MS/MS analysis. The mass spectrometric analysis identified 51 parasite proteins (Table S2). After excluding 35 proteins lacking both a signal peptide sequence and transmembrane region, the list contained two core PTEX components, EXP2 and PTEX150; one PTEX-associated protein, Pf113; and eight iRBC-exported proteins, including REX1, SBP1, Pf332, MAHRP1, and four PEXEL-positive uncharacterized exported proteins (Table 2). The remaining three proteins were a putative transmembrane emp24 domain-containing protein (PF3D7_1308400), a conserved *Plasmodium* protein with unknown function (PF3D7_1308400), and a putative thioredoxin-related protein. The last protein has a signal peptide sequence followed by a Pfam thioredoxin domain, a transmembrane region, and a short cytoplasmic tail, similar to Trx2 except that Trx2 does not possess a transmembrane region. It would be interesting to explore the possibility that this thioredoxin domain-containing protein plays a role on behalf of Trx2 for membrane proteins in the PV space.

Table 1
Selected *P. falciparum* proteins identified from immunoprecipitated materials with mini-SURFIN$_{4.1}$.

	Annotation	Gene ID	Experiment 1 Quantitative value		Experiment 2 Quantitative value		Features
			Parental line (control)	mini-SURFIN$_{4.1}$	TyGFP (control)	mini-SURFIN$_{4.1}$	
PTEX component							
1	Heat shock protein 101 (HSP101)	PF3D7_1116800	0	7	0	1	Signal peptide (+)
2	Exported protein 2 (EXP2)	PF3D7_1471100	0	3	0	1	Signal peptide (+)
3	Translocon component PTEX150 (PTEX150)	PF3D7_1436300	0	3	0	0	Signal peptide (+)
Other proteins with PVM, PPM, or PV localization							
4	Parasitophorous vacuolar protein 1 (PV1)	PF3D7_1129100	0	5	0	1	Signal peptide (+)
5	Early transcribed membrane protein 10.2 (ETRAMP10.2)	PF3D7_1033200	0	4	0	2	Signal peptide (+), one TM region
6	Early transcribed membrane protein 5 (ETRAMP5)	PF3D7_0532100	0	2	0	0	Signal peptide (+), one TM region
7	Pf113	PF3D7_1420700	0	1	0	2	Signal peptide (+), GPI-anchor (+)
8	Sexual stage-specific protein precursor (Pfs16)	PF3D7_0406200	0	1	0	0	Signal peptide (+), one TM region
9	Early transcribed membrane protein 10.1 (ETRAMP10.1)	PF3D7_1001500	0	1	0	0	Signal peptide (+), one TM region
10	Early transcribed membrane protein 4 (ETRAMP4)	PF3D7_0423700	0	1	0	0	Signal peptide (+), one TM region
11	Exported protein 1 (EXP1)	PF3D7_1121600	0	1	0	0	Signal peptide (+), one TM region
12	Exported protein 3 (EXP3)	PF3D7_1024800	0	1	0	0	Signal peptide (+), one TM region
13	Non-SERCA-type Ca2+ − transporting P-ATPase (ATP4)	PF3D7_1211900	0	1	0	0	Eight TM regions
14	Niemann-Pick type C1-related protein (NCR1)	PF3D7_0107500	0	1	0	0	Twelve TM regions
Exported to iRBC cytoplasm							
15	Skeleton-binding protein 1 (SBP1)	PF3D7_0501300	0	3	0	0	One TM region (PNEP)
16	PEXEL-negative exported protein	PF3D7_0830400	0	2	0	0	Signal peptide (+), one TM region (PNEP)
17	Ring-exported protein 1 (REX1)	PF3D7_0935900	0	1	0	1	One TM region (PNEP)
18	Glycophorin binding protein 130 (GBP130)	PF3D7_1016300	0	1	0	1	PEXEL motif (+), one TM region
19	EMP1-trafficking protein (PTP1)	PF3D7_0202200	0	1	0	0	PEXEL motif (+), two TM regions
20	Small exported membrane protein 1 (SEMP1)	PF3D7_0702400	0	1	0	0	One TM region (PNEP)
21	*Plasmodium* exported protein, unknown function	PF3D7_0301700	0	1	0	0	PEXEL motif (+), two TM regions
Rhoptry localization							
22	Rhoptry neck protein 3 (RON3)	PF3D7_1252100	0	1	0	0	Signal peptide (+), three TM regions
23	High molecular weight rhoptry protein 2 (RhopH2)	PF3D7_0929400	0	1	0	0	Signal peptide (+)
24	High molecular weight rhoptry protein 3 (RhopH3)	PF3D7_0905400	0	1	0	0	Signal peptide (+)
Unknown localization							
25	Major facilitator superfamily-related transporter (MFR4)	PF3D7_0914700	0	2	0	1	Ten TM regions
26	Major facilitator superfamily-related transporter (MFR5)	PF3D7_1129900	0	1	0	1	Twelve TM regions
27	Thioredoxin-related protein, putative	PF3D7_1352500	0	1	0	0	Signal peptide (+), one TM region
28	Conserved *Plasmodium* protein, unknown function	PF3D7_0811600	0	1	0	0	Signal peptide (+)
29	Conserved *Plasmodium* protein, unknown function	PF3D7_0721100	0	1	0	0	Signal peptide (+)
30	Conserved *Plasmodium* protein, unknown function	PF3D7_0706100	0	1	0	0	Signal peptide (+)

Signal peptides were predicted using SignalP v3 (Bendtsen et al., 2004). Transmembrane (TM) regions were predicted using TMHMM v2 (Krogh et al., 2001) and those predicted as signal peptide sequences were excluded. GPI-anchor attachment sites were predicted by big-PI predictor. The presence of PEXEL/PEXEL-like motifs is according to previous reports (Marti et al., 2004; Schulze et al., 2015). PNEP, PEXEL-negative exported protein.

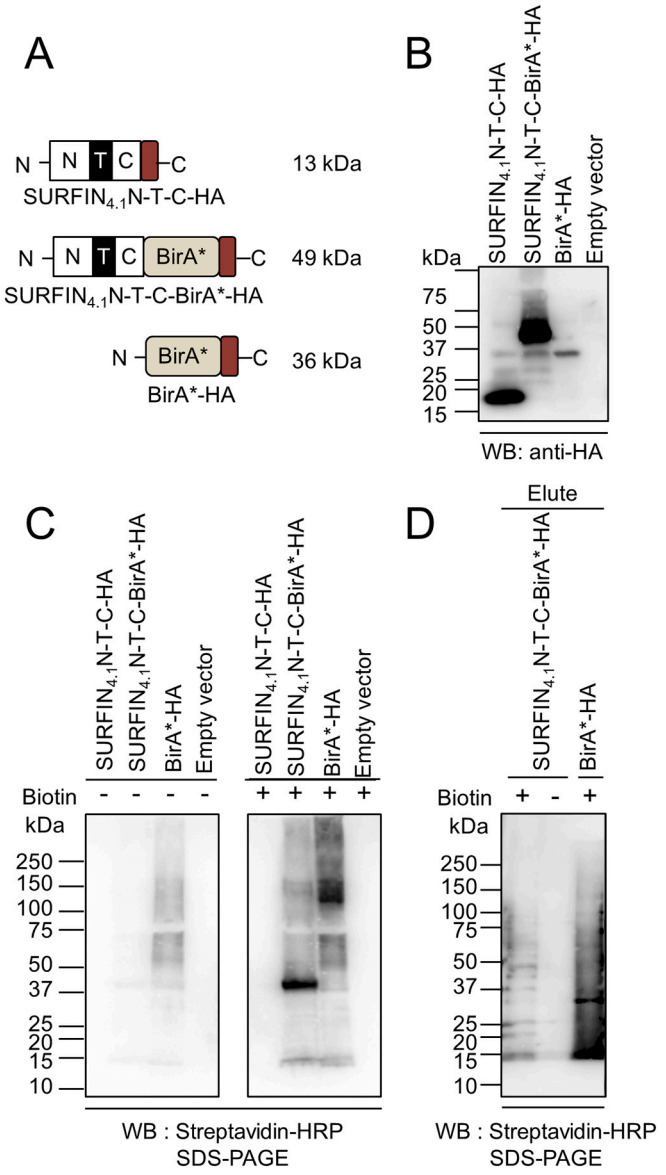

Fig. 2. BioID to identify proteins interacting with the SURFIN$_{4.1}$N-T-C region. (A) Schematic representations of the BirA* and HA-fused SURFIN$_{4.1}$-N-T-C region (SURFIN$_{4.1}$N-T-C-BirA*-HA) and control proteins (SURFIN$_{4.1}$N-T-C-HA and BirA*-HA). BirA* is a mutated biotin ligase and HA is a hemagglutinin tag. The expected size of each protein is indicated. (B) Western blot (WB) analysis of parasite proteins solubilized from transgenic parasites expressing SURFIN$_{4.1}$N-T-C-BirA*-HA or from control parasites with anti-HA. A parasite transfected with a vector plasmid backbone only was used as a negative control (Empty vector). (C) Biotinylation of parasite proteins in transfectants expressing SURFIN$_{4.1}$N-T-C-BirA*-HA or in control parasites. Biotinylated proteins were visualized by Western blotting using streptavidin-conjugated horseradish peroxidase (streptavidin-HRP) and its substrate. Proteins were extracted from parasites cultured with biotin (right panel) or without biotin (left panel). Smear bands for the BirA*-HA sample without biotin is likely due to the biotinylation of parasite proteins with endogenous biotin in the cell culture. (D) Western blotting with streptavidin-HRP for the fractions solubilized then purified from transfectants expressing SURFIN$_{4.1}$N-T-C-BirA*-HA treated with biotin using streptavidin beads. Biotinylated proteins from control parasites expressing BirA*-HA cultured with or without biotin were also assessed.

HSP101 was not identified, which may be due to the low abundance of peptide or that the biotinylation site was far from the BirA* region.

3.3. Immunoprecipitation followed by specific antibody detection confirmed that mini-SURFIN$_{4.1}$ interacted with three core PTEX components and Pf113

Interaction of SURFIN$_{4.1}$ with PTEX components and Pf113 was indicated by two approaches in this study, and we therefore sought additional validation of their interaction. To characterize Pf113, we raised mouse and rabbit antibodies against Pf113 (Fig. 3A). We sequentially solubilized parasite proteins under stringent conditions with SDS, because Pf113 was identified as a detergent-resistant membrane (DRM)-resident protein [55,56]. Western blotting with anti-Pf113 serum under a reducing condition detected several bands around ~250 kDa, ~150 kDa, ~100 kDa, and ~ 60 kDa (Fig. 3B). Given that the expected full length of Pf113 is 113 kDa, the bands smaller than the expected size are possibly derived from processed or degradation products. The ~250 kDa band may be derived from an SDS-resistant multimeric form of Pf113 or a protein complex with unknown interacting proteins, in agreement with published observations [57].

Immunoprecipitated fractions with anti-Ty1 from the parasite expressing mini-SURFIN$_{4.1}$ or TyGFP were probed with anti-EXP2, anti-HSP101, anti-PTEX150, or anti-Pf113, and corresponding bands were detected predominantly from the parasite expressing mini-SURFIN$_{4.1}$ (Fig. 4A–C). For Pf113, only an ~250-kDa band was detected. We also detected smear bands around 1000 kDa from the parasite expressing mini-SURFIN$_{4.1}$ with anti-EXP2, anti-HSP101, and anti-Pf113 by electrophoresis using NativePAGE Bis-Tris Gel (Fig. 4A–C).

Reciprocal immunoprecipitation using lysates of transfectant expressing mini-SURFIN$_{4.1}$ revealed the existence of mini-SURFIN$_{4.1}$ in all fractions immunoprecipitated with anti-EXP2, anti-HSP101, anti-PTEX150, or anti-Pf113 (Fig. 4D and E). These four proteins were additionally detected in the fractions immunoprecipitated with anti-EXP2, anti-HSP101, anti-PTEX150, or anti-Pf113 (Fig. 4D and E), suggesting that mini-SURFIN$_{4.1}$ interacts with PTEX and Pf113 and results in the formation of high molecular weight protein complexes.

3.4. Pf113 localized to the merozoite apical end in the segmented schizonts and the parasite periphery after RBC invasion

Three core PTEX components, EXP2, HSP101, and PTEX150, localize to merozoite dense granules at the schizont stage [23] and are released to the parasitophorous vacuole space during merozoite invasion [58]. To explore if Pf113 is also a dense granule protein, we performed IFA using antibodies against Pf113 in combination with marker proteins for secretion organelles. Pf113 signal was observed at the late schizont stage and co-localized with a dense granule marker protein RESA, but not with the microneme marker protein AMA1, or the rhoptry body and neck marker proteins RAP1 and RON2, respectively (Fig. 5); supporting that Pf113 is a dense granule protein.

To determine the localization of Pf113 after RBC invasion and its spatial association with the PTEX complex on the parasite periphery, we performed IFA using anti-Pf113 and anti-EXP2, anti-HSP101, or anti-PTEX150 under acetone fixation conditions. At the ring and late trophozoite stages, Pf113 signal was observed on the parasite periphery and in most cases co-localized with signals of core PTEX components (Fig. 6A–C), suggesting PPM or PVM location. SR-SIM imaging data also indicated parasite peripheral location of Pf113; which were, partially co-localized with EXP2 signals (Fig. 6D), suggesting that the complex formation of these proteins is temporal. Nonetheless, these observation are consistent with a study showing Pf113 co-localized with EXP1, a marker of PVM protein at the trophozoite stage [57].

Next, we performed IFA with antibodies against a Ty1 tag and EXP2 using a transfectant expressing mini-SURFIN$_{4.1}$. We observed co-localization of Ty1 signal and EXP2 or Pf113 signal on the parasite

Table 2
Selected *P. falciparum* proteins identified by the BioID method.

	Annotation	Gene ID	Experiment 3 (BioID) Quantitative value		Features
			BirA*-HA (control)	$SURFIN_{4.1}$N-T-C-BirA*-HA	
PTEX component					
1	Exported protein 2 (EXP2)	PF3D7_1471100	0	2	Signal peptide (+)
2	Translocon component PTEX150 (PTEX150)	PF3D7_1436300	0	1	Signal peptide (+)
Other proteins with PVM, PPM, or PV localization					
3	Pf113	PF3D7_1420700	0	2	Signal peptide (+), GPI-anchor (+)
Exported to the iRBC cytoplasm					
4	Ring-exported protein 1 (REX1)	PF3D7_0935900	0	5	One TM region (PNEP)
5	Skeleton-binding protein 1 (SBP1)	PF3D7_0501300	0	3	One TM region (PNEP)
6	Membrane associated histidine-rich protein (MAHRP1)	PF3D7_1370300	0	2	One TM region (PNEP)
7	Antigen 332, DBL-like protein (Pf332)	PF3D7_1149000	0	2	Signal peptide (+), one TM region (PNEP)
8	*Plasmodium* exported protein, unknown function	PF3D7_0831400	0	2	Signal peptide (+), PEXEL motif (+)
9	*Plasmodium* exported protein, unknown function	PF3D7_0501000	0	1	PEXEL motif (+), one TM region
10	*Plasmodium* exported protein (hyp16), unknown function (PfJ23)	PF3D7_1001900	0	1	PEXEL motif (+), three TM regions
11	*Plasmodium* exported protein (PHISTb), unknown function	PF3D7_1201000	0	1	Signal peptide (+), PEXEL motif (+)
Unknown localization					
12	Thioredoxin-related protein, putative	PF3D7_1352500	0	1	Signal peptide (+), one TM region
13	Conserved *Plasmodium* protein, unknown function	PF3D7_1308400	0	1	Three TM regions
14	Transmembrane emp24 domain-containing protein, putative	PF3D7_0422100	0	1	Signal peptide (+), one TM region

Signal peptides were predicted using SignalP v3 (Bendtsen et al., 2004). Transmembrane (TM) regions were predicted using TMHMM v2 (Krogh et al., 2001) and those predicted as signal peptide sequences were excluded. GPI-anchor attachment sites were predicted by big-PI predictor. The presence of PEXEL/PEXEL-like motifs is according to previous reports (Marti et al., 2004; Schulze et al., 2015). PNEP, PEXEL-negative exported protein.

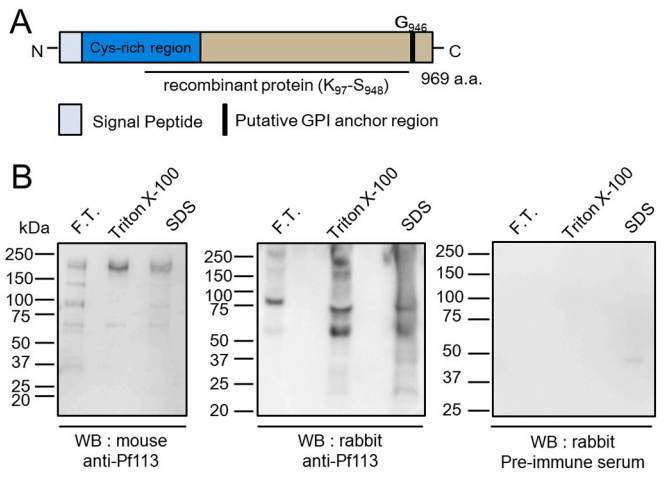

Fig. 3. Western blotting with antibody against Pf113. (A) Schematic representation of the Pf113 protein in *P. falciparum*. Pf113 consists of a signal peptide (M_1–C_{22}), cysteine-rich domain (Y_{23}–K_{219}), and a predicted GPI-anchor modification site (G_{946}). The region spanning K_{97} to S_{948} was used to generate a recombinant protein. (B) Western blotting with anti-Pf113 (mouse and rabbit, left and middle, respectively) against parasite proteins sequentially extracted from transfectants expressing mini-$SURFIN_{4.1}$. The freeze-thaw (F.T.) fraction contained soluble proteins. After extraction of soluble proteins, parasite pellets were further solubilized with 1% Triton X-100, and then with 2% SDS to completely extract integral membrane proteins. Western blotting with a control pre-immune rabbit serum (right panel) indicates only faint background staining in the SDS-fraction.

periphery (Fig. 6E and F), which was consistent with the detected interaction between mini-$SURFIN_{4.1}$ and PTEX components by biochemical analyses. Dotted mini-$SURFIN_{4.1}$ signals in the RBC cytoplasm were previously confirmed to localize to Maurer's clefts [33], where mini-$SURFIN_{4.1}$ might interact with other exported proteins detected by biochemical analyses. Altogether, our microscopic analysis indicated parasite peripheral and dense granule localization of Pf113 (Fig. 6G).

3.5. *Pf113 is a component of a stable translocation intermediate complex with export-arrested mini-$SURFIN_{4.1}$*

Export-arrested SBP1 has been shown to form a stable translocation intermediate complex with the EXP2 pore component [21]. We were interested in determining if export-arrested mini-$SURFIN_{4.1}$ forms a stable translocation intermediate complex and its link with PTEX and Pf113. We generated a transfectant expressing the $SURFIN_{4.1}$N-T-C region fused with murine dihydrofolate reductase (mDHFR) and a TyGFP tag (mini-$SURFIN_{4.1}$-mDHFR) and control protein (Fig. 7A). The binding of mDHFR to the drug WR99210 stabilizes the protein and its unfolding is inhibited [19], thus protein unfolding of exported mDHFR-fused proteins can be regulated by addition of WR99210. We confirmed the protein expression by Western blotting with anti-Ty1 in each transfectant including the control line (Fig. S4A). Our IFA analysis also confirmed that mini-$SURFIN_{4.1}$-mDHFR accumulated in the parasite cytoplasm and was not trafficked to the iRBC cytoplasm in the presence of WR99210 (Fig. S4B) and this inhibition was dependent on the tagged mDHFR (Fig. S4B). We found that the export block by WR99210 does not affect the replication of the transgenic parasite (Fig. S4C).

Next, we tried to detect high molecular weight protein complexes from the lysate of a parasite expressing export-arrested mini-$SURFIN_{4.1}$-mDHFR without any chemical cross-linking. We detected an ~160-kDa protein complex by BN-PAGE with anti-Ty1, whereas control mini-$SURFIN_{4.1}$ forms an ~200-kDa protein complex like that observed in our previous experiment (Fig. S4D). This suggests that mDHFR tagging affects interaction of $SURFIN_{4.1}$with the components of the protein complex.

To isolate the stable translocation intermediate complex, we performed chemical cross-linking and immunoprecipitation with anti-Ty1. Both in the presence or absence of WR99210, we detected EXP2, but not HSP101 and PTEX150, in the immunoprecipitated fraction from parasites expressing mini-$SURFIN_{4.1}$-mDHFR (Fig. 7B). This contrasts with our observation for parasites expressing mini-$SURFIN_{4.1}$ without a mDHFR domain, for which EXP2, HSP101, and PTEX150 were detected (Fig. 4). Western blotting with anti-Pf113 in the immunoprecipitated

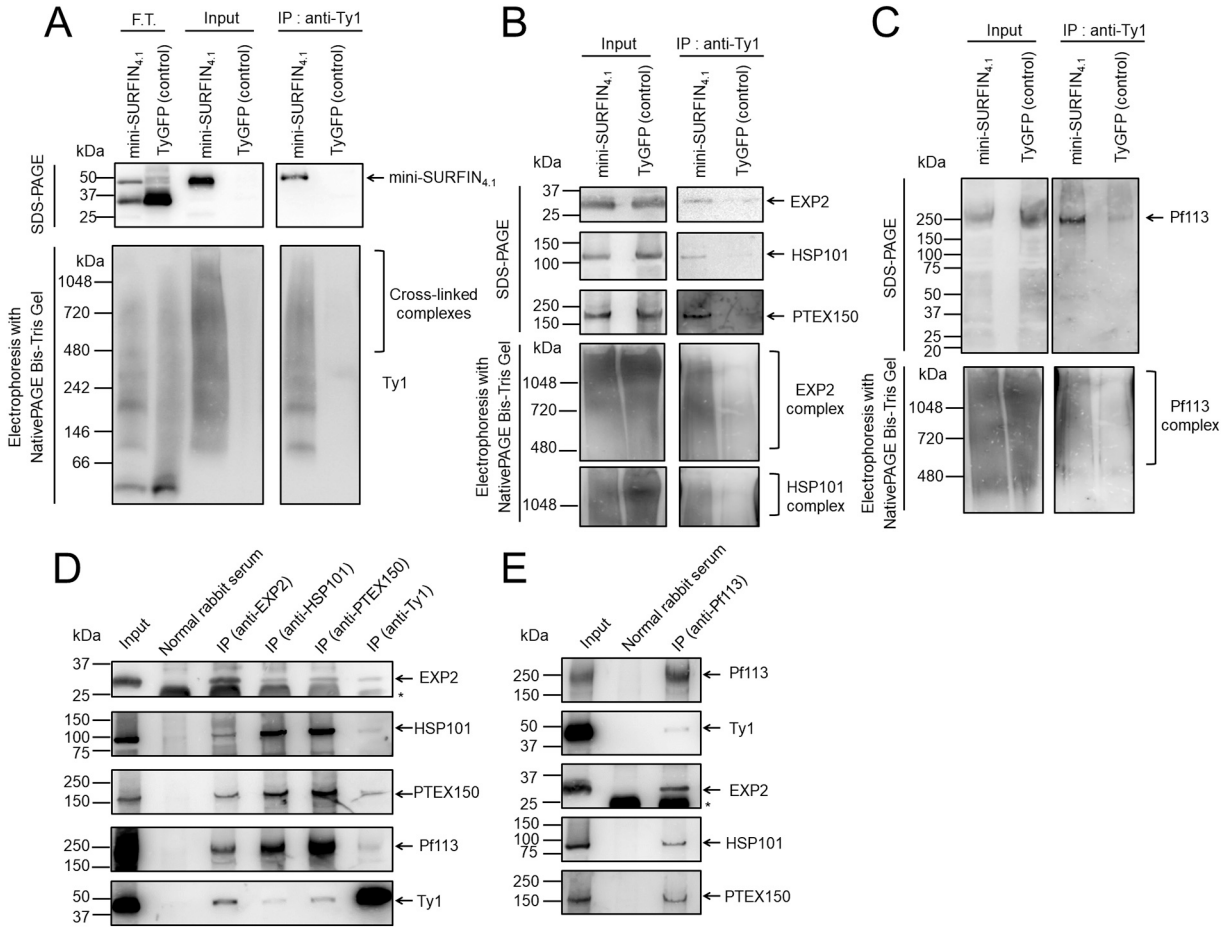

Fig. 4. mini-SURFIN$_{4.1}$ forms a protein complex with core PTEX components and Pf113. (A) Immunoprecipitation from the transfectant expressing Ty1-tagged mini-SURFIN$_{4.1}$ or a control protein TyGFP with anti-Ty1. The freeze-thaw (F.T.) fraction, the solubilized fraction with 2% SDS and 0.5% Triton X-100 after removing F.T. fraction (Input), and the immunoprecipitated (IP) fraction with anti-Ty1 from the solubilized fraction were subjected to SDS-PAGE or NativePAGE gel electrophoresis followed by Western blotting with anti-Ty1. Mini-SURFIN$_{4.1}$ was detected in both the input and IP fraction (arrow). TyGFP control protein was extracted in the F.T. fraction because it is a soluble protein. (B) Co-precipitation of three core PTEX components by IP with anti-Ty1 from the transfectant expressing Ty1-tagged mini-SURFIN$_{4.1}$. Input and IP fraction were subjected to SDS-PAGE or NativePAGE gel electrophoresis followed by Western blotting with anti-EXP2, anti-HSP101, or anti-PTEX150. (C) Western blotting with anti-Pf113 showing co-precipitation of Pf113 with Ty1-tagged mini-SURFIN$_{4.1}$. The ~250-kDa form of Pf113 was detected in the IP fraction after SDS-PAGE (top) and smeared bands indicating high weight protein complexes by NativePAGE Bis-Tris gel electrophoresis (bottom). (D) Reciprocal IP using anti-EXP2, anti-HSP101, or anti-PTEX150 to purify protein complexes consisting of three core PTEX components and mini-SURFIN$_{4.1}$. Input and IP fractions with each antibody were applied to SDS-PAGE then probed with anti-EXP2, anti-HSP101, anti-PTEX150, or anti-Ty1 (arrow). (E) Reciprocal IP with anti-Pf113 rabbit serum, confirmed the interaction of an ~250-kDa form of Pf113 with three core PTEX components, and mini-SURFIN$_{4.1}$. Mouse anti-Pf113 was used to detect Pf113 on the membranes. Normal rabbit serum was used as a negative control for IP. An asterisk indicates a band originating from an immunoglobulin light chain derived from the antibody used for immunoprecipitation.

fraction from parasites expressing mini-SURFIN$_{4.1}$-mDHFR showed increased intensity of an ~60 kDa band by addition of WR99210 (Fig. 7B), whereas the band intensity of Pf113 at ~250 kDa in the immunoprecipitated fraction from parasites expressing mini-SURFIN$_{4.1}$ is similar with and without WR99210 (Fig. 7C). This ~60 kDa band is consistent with the band detected in Western blotting with anti-Pf113 in this study (Fig. 3C). These results suggest that mDHFR tagging disrupts the integrity of the PTEX complex with mini-SURFIN$_{4.1}$ and that the stable translocation intermediate complex contains an ~60 kDa form of Pf113.

4. Discussion

Here we performed biochemical analyses to identify the components of a translocation intermediate using mini-SURFIN$_{4.1}$ as a probe. We have shown that three core PTEX components and Pf113 comprise a translocation intermediate complex. Our data provides further insight into the translocation model of integral membrane proteins in the *P. falciparum* PPM as well as PVM, which could aid the discovery of an unidentified PPM translocon.

Given that SURFIN$_{4.1}$ interacted with three core PTEX components, EXP2, HSP101, and PTEX150, as well as Pf113, we propose that these proteins comprise a native form of a translocation intermediate complex for trafficking of integral membrane protein to the RBC (Fig. 8A). Mesén-Ramírez et al. (2016) identified a "stable translocation intermediate complex" composed of the EXP2 pore and clogged exported proteins tagged with mDHFR [21]. In their study, however, the interaction of the export substrate with other PTEX component HSP101 was not detected in the stable translocation intermediate complex and involvement of PTEX150 was also unclear. This is consistent with our results that only EXP2 but not HSP101 and PTEX150 were co-precipitated with export-arrested mini-SURFIN$_{4.1}$-mDHFR, suggesting that mDHFR tagging is detrimental to the stability of the native form of the translocation intermediate (Fig. 8B). A recent study revealed that when its unfolding was inhibited an mDHFR-fused soluble protein co-localized with EXP2, and not HSP101 and PTEX150, at loop-like structures extending from

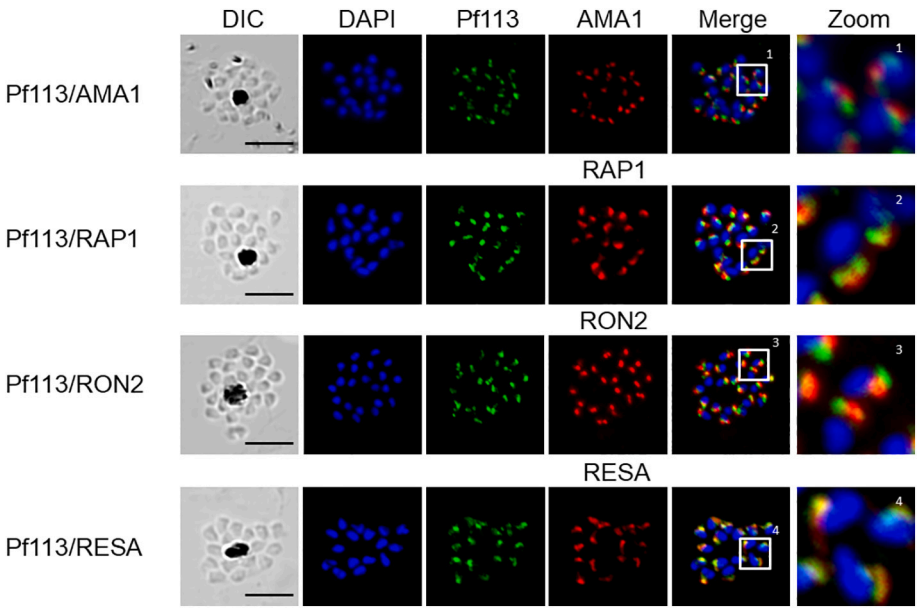

Fig. 5. Pf113 is localized in dense granules at the schizont stage. Segmented schizonts were co-stained with antibodies specific to Pf113 and either RESA (dense granule marker), AMA1 (microneme marker), RAP1 (rhoptry body marker), or RON2 (rhoptry neck marker). Co-localization of Pf113 with RESA, but not others, in the merged image suggests that Pf113 is a dense granule protein. Boxed areas labeled 1 to 4 in the merged images indicate zoomed areas shown in the rightmost panels. Parasite nuclei were stained with DAPI (blue). DIC; differential interference contrast microscopy image. Scale bars = 5 μm. (For interpretation of the references to colour in this figure legend, the reader is referred to the web version of this article.)

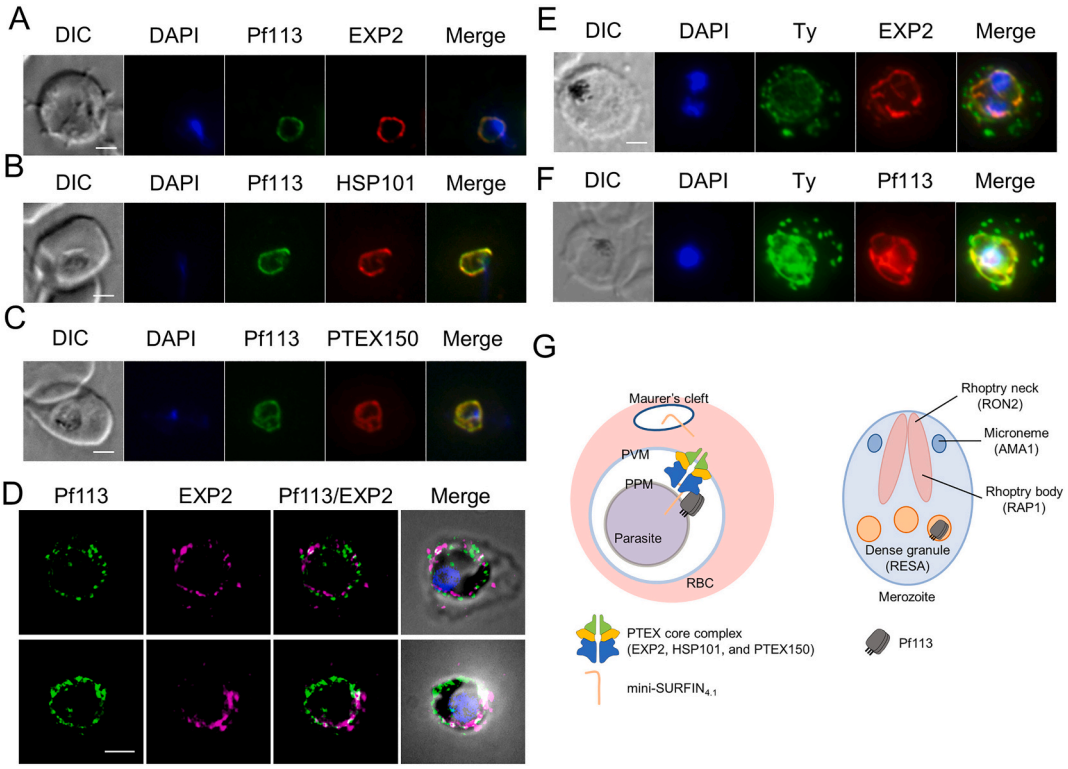

Fig. 6. Pf113 localizes at the parasite periphery at the trophozoite stage. (A) Double staining IFA with anti-Pf113 and anti-EXP2, (B) with anti-HSP101, or (C) with anti-PTEX150. Co-localization of Pf113 with three core PTEX components (EXP2, HSP101, and PTEX150) suggests the presence of Pf113 on the PPM or PVM. (D) Blood smears were co-stained with anti-Pf113 (green) and anti-EXP2 (purple). Pf113 signals were detected at the parasite periphery, and only partially co-localized with the EXP2 signal, suggesting that the complex formation of these two proteins is temporal. (E, F) Double staining IFA with anti-Ty1 and anti-EXP2 (E) or with anti-Pf113 (F). In addition to the dotted Ty1 signals in the iRBC cytoplasm, Ty1 signals on the parasite periphery co-localize with EXP2 or Pf113 signals. (G) Schematic representations of Pf113 localization in the RBCs. Blood smears were fixed with acetone and parasite nuclei were stained with DAPI (blue). DIC; differential interference contrast microscopy image. Scale bars = 2 μm. (For interpretation of the references to colour in this figure legend, the reader is referred to the web version of this article.)

the PVM [27]. This observation is consistent with our study. However, HSP101 and PTEX150 might be dissociated from the complex during the purification procedure; because these components were not detected even under the condition when mini-SURFIN$_{4.1}$-mDHFR was exported to the RBC without WR99210. Another recent study has described a PfEMP1 interactome, suggesting interaction of PTEX components and PfEMP1 [32]. In that study all five components of PTEX were identified as mini-PfEMP1 interacting proteins, but interaction of Pf113 and

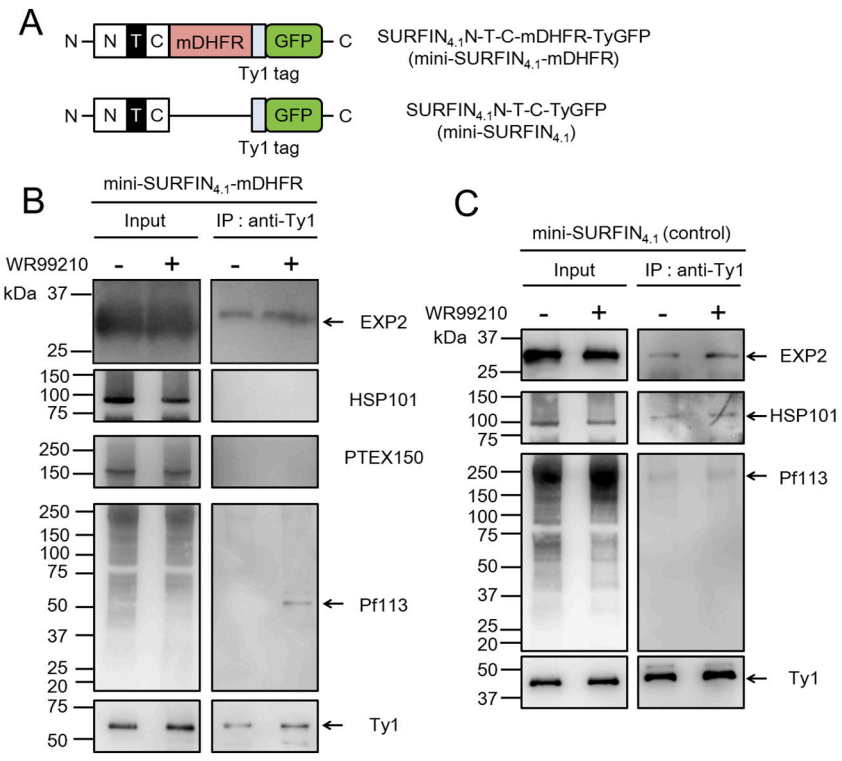

Fig. 7. Export-arrested mini-SURFIN$_{4.1}$ forms a stable translocation intermediate complex with Pf113 and EXP2. (A) Schematic representations of mini-SURFIN$_{4.1}$ fused with mDHFR or a control mini-SURFIN$_{4.1}$ expressed in the transfectants. The mini-SURFIN$_{4.1}$ composition is described in the Fig. 1 legend. A Ty1 tag was used for immunoprecipitation and Western blotting. (B) Immunoprecipitation (IP) of mini-SURFIN$_{4.1}$-mDHFR (C) or control mini-SURFIN$_{4.1}$ using anti-Ty1. Input and IP fraction with anti-Ty1 were subjected to Western blotting with anti-EXP2, anti-HSP101, anti-PTEX150, anti-Pf113, or anti-Ty1. Arrows indicate each target protein. An ~60-kDa form of Pf113 was co-precipitated with mini-SURFIN$_{4.1}$-mDHFR when export was arrested with WR99210. EXP2, but not other core PTEX components HSP101 and PTEX150, was co-precipitated with mini-SURFIN$_{4.1}$-mDHFR with or without WR99210. (C) Core PTEX components EXP2 and HSP101, and an ~250-kDa form of Pf113 were co-precipitated with control mini-SURFIN$_{4.1}$ in the presence or absence of WR99210.

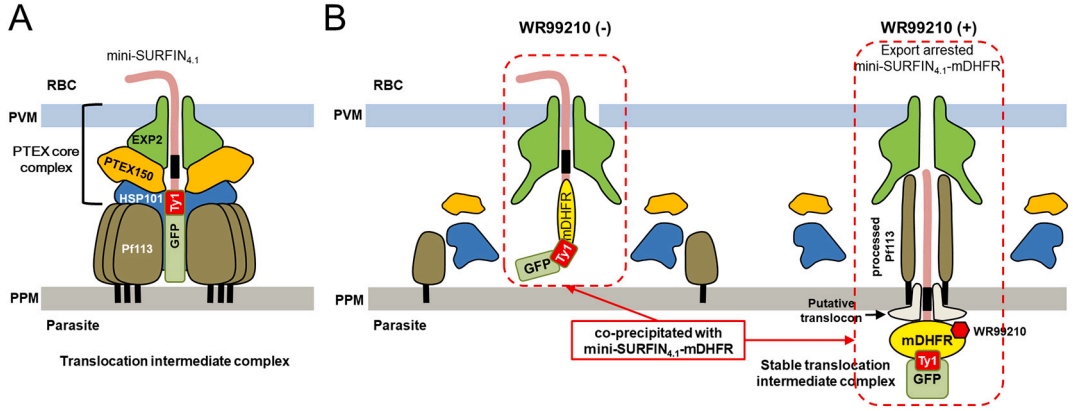

Fig. 8. Model of the translocation of mini-SURFIN$_{4.1}$. (A) Schematic of the translocation intermediate complex with mini-SURFIN$_{4.1}$. PTEX150 and HSP101 are in the same complex with the EXP2 pore complex and mini-SURFIN$_{4.1}$. The ~250-kDa form of Pf113 interacts with core PTEX components. (B) Schematics of the translocation intermediate complex with mini-SURFIN$_{4.1}$-mDHFR protein in the absence (left) or presence (right) of WR99210. Export-arrested mini-SURFIN$_{4.1}$-mDHFR accumulated on the parasite plasma membrane and forms a stable translocation intermediate complex. A potential component is an ~60-kDa cleaved product of Pf113. This intermediate complex is distinctive from the PTEX core complex. A putative translocon on parasite plasma membrane is shown.

PfEMP1 was not shown [32]. In contrast to their study, we clearly demonstrated that mini-SURFIN$_{4.1}$, Pf113, and three core PTEX components exist as a protein complex. This difference might be derived from variant experimental conditions such as solubilization steps, chemical cross-linking, or expression level of bait exported proteins. Alternatively, Pf113 may not be involved in the translocation of PfEMP1. Investigating the interaction of Pf113 with other integral membrane proteins, such as PfEMP1, would be useful to make a general translocation model for integral membrane proteins.

Interaction of HSP101 with mini-SURFIN$_{4.1}$ protein may facilitate the transport of the cargo by threading into the EXP2 pore complex rather than unfolding in the PV. A recent study using a variety of transgenic *P. berghei* lines suggests that partially functional HSP101, which possesses threading motor activity but not unfolding activity, can support efficient transport of PbCP1, an integral membrane protein containing a PEXEL motif [20]. This model implied a prior unfolding of exported integral membrane proteins before they reach the PV, achieved by a mechanism in which unidentified proteins in the PPM or unfolding during vesicular trafficking are involved.

We have identified several parasitophorous vacuole or PVM-resident SURFIN$_{4.1}$ interacting proteins that are potentially involved in the translocation of integral membrane proteins. PV1, a protein identified by our study, was shown to interact with PTEX150, and contribute to the trafficking of PfEMP1, suggesting that PV1 is a component of a novel protein trafficking machinery [32,52]. In addition, PV1 can interact with PTP5, a soluble PEXEL exported protein, for its trafficking to the RBC [59]. Although we did not confirm interaction of mini-SURFIN$_{4.1}$ and PV1, this protein may function in translocation for integral

membrane proteins such as SURFIN$_{4.1}$ and PfEMP1. Other candidates potentially involved in the translocation step include ETRAMPs, PVM-resident single transmembrane proteins encoded in a multigene family [60]. ETRAMP$_{10.2}$ was shown to form an ~140-kDa protein complex in DRM fractions [56]. One subtype of ETRAMP has the property to oligomerize in the PVM [60]. ETRAMP$_{10.2}$ oligomers may therefore be cross-linked with mini-SURFIN$_{4.1}$ and form high molecular weight protein complexes. The ETRAMP complex potentially functions in the translocation step of integral membrane proteins, but this hypothesis remains to be clarified in further studies. A panel of exported proteins were also co-precipitated with mini-SURFIN$_{4.1}$. These proteins are likely translocated across the PVM through the PTEX translocon independently of each other, thus we consider that these exported proteins might interact with mini-SURFIN$_{4.1}$ during trafficking to or at the Maurer's clefts, directly or indirectly.

We propose that PTEX, Pf113, and exported integral membrane proteins form a protein complex within a specific microdomain such as a DRM on the parasite periphery. Two independent DRM proteomic analyses detected PTEX and Pf113 [56,57]. Pf113 and mini-SURFIN$_{4.1}$ are not fully solubilized with the non-ionic detergent Triton X-100 and require the ionic detergent SDS for complete solubilization. This result supports the concept that the Pf113 complex exists in a DRM. DRM-resident PTEX and Pf113 may be cooperatively involved in translocation of integral membrane proteins to the human RBC.

We demonstrated that Pf113 showed co-localization with dense granule protein, RESA, at the schizont stage and parasite peripheral localization at the trophozoite stage. It has been shown that PTEX components are immediately released from dense granules during invasion [58]. PV1, a PTEX associated protein, was recently shown to localize to dense granules [59], and Pf113 is likely secreted similarly. During the ring and late trophozoite stages, clear co-localization of PTEX components and Pf113 was observed, suggesting that Pf113 interacts with other PTEX components and forms a protein complex on the parasite periphery during intraerythrocytic development. Our data favor the concept that Pf113 plays a role in protein transport, rather than in RBC invasion, which was proposed by a study showing that Pf113 binds to one of the invasion ligands, Rh5 [61].

It will be interesting to evaluate the roles of Pf113 in *P. falciparum* life cycle stages other than the asexual blood stage, because the Pf113 ortholog in the rodent malaria parasite *P. berghei* contributes not to blood stage development, but to the conversion of sporozoites to the liver stage [62]. A recent genetic screening analysis using a transposon also indicated that Pf113 can be disrupted at the asexual blood stage in vitro [63]. Thus, Pf113 may play an auxiliary role in protein transport to iRBC cytoplasm. Pf113 transcripts are detectable in *P. falciparum* matured gametocytes [64], oocysts, and sporozoites [65], which is consistent with the ubiquitous expression of the Pf113 ortholog in *P. berghei* and this implies potential roles in the mosquito and liver stages [62].

We did not observe a growth defect of the transfectant expressing mini-SURFIN$_{4.1}$-mDHFR in the presence of WR99210. Mesén-Ramírez et al. (2016) suggested that the amino acid length between the transmembrane region and the mDHFR reporter region is critical to reach and to be clogged at the PTEX translocon; in the case of the mDHFR-fused SBP1 protein, it was 99 amino acids and protein export was blocked, whereas in the case of the mDHFR-fused REX2 protein it was 34 amino acids and the export was not blocked [21]. Our result is consistent with this report, because the length between the transmembrane region and the mDHFR region in our mini-SURFIN$_{4.1}$-mDHFR is only 28 amino acids, which would not block the export of other proteins across the PVM, and thus not affect parasite growth.

Our biochemical data suggests that mini-SURFIN$_{4.1}$-mDHFR is possibly clogged at the PPM when export was arrested with WR99210, which in turn might enhance the interaction between arrested mini-SURFIN$_{4.1}$-mDHFR and an ~60-kDa Pf113 product (Fig. 8B). The ~60-kDa Pf113 product is potentially cleaved in the PV and may support the function of an unidentified PPM translocon for exported integral membrane proteins such as SURFIN$_{4.1}$. Among three PTEX core complex components, only EXP2 was detected in the stable translocation intermediate complex with export-arrested mini-SURFIN$_{4.1}$-mDHFR. Together with the lack of a growth defect with WR99210, this suggests that export-arrested mini-SURFIN$_{4.1}$-mDHFR may be recruited to the EXP2 pore and indirectly interacts with EXP2 via Pf113 or unknown factors.

In conclusion, this study provides biochemical evidence for a translocation intermediate complex composed of integral membrane proteins. This is the first report showing interaction of an exported integral membrane protein and Pf113, a PTEX-associated uncharacterized protein. Reverse genetic approaches will contribute to characterize the role of Pf113 in trafficking of integral membrane proteins. Characterizing the whole biochemical composition of the translocation complex with a soluble and an integral membrane protein would clarify if Pf113 is only involved in the translocation of integral membrane proteins. Understanding the mechanistic framework of translocation is essential to reveal protein trafficking mechanisms in malaria parasites and to provide new targets of anti-malarial drugs.

Data availability

The datasets presented in this study can be found in the online repository jPOST (Okada et al., 2017) with the accession number of PXD023028 for ProteomeXchange and JPST001028 for jPOST.

Funding

This work was supported in part by Grants-in-Aids for Scientific Research on Innovative Areas 23117008, MEXT, Japan (OK, TT) and by the Tokyo Biochemical Research Foundation 13-B1-8 (SM) and GlaxoSmithKline Japan research grant (SM). BYAC was supported by the leading program, Nagasaki University, Japan. ABL was a recipient of MEXT Ph.D. scholarship, Japan. This work was conducted at the Joint Usage/Research Center on Tropical Disease, Institute of Tropical Medicine, Nagasaki University. The funders had no role in study design, data collection and analysis, decision to publish, or preparation of the manuscript.

Declaration of Competing Interest

The authors declare that this study received funding from GlaxoSmithKline Japan. The funder was not involved in the study design, collection, analysis, interpretation of data, the writing of this article, or the decision to submit it for publication.

Acknowledgements

We are grateful to the Nagasaki Red Cross Blood Center for providing human RBC and plasma. We thank M. Takeda, R. Tanaka, M. Sakura, S. Takahama, and N. Matsumoto for technical assistance. We also thank T. J. Templeton for critical reading of the manuscript. We would also like to thank N. E. Sherman, W. M. Keck Biomedical Mass Spectrometry Laboratory, University of Virginia, USA for mass spectrometric analysis.

Appendix A. Supplementary data

Supplementary data to this article can be found online at https://doi.org/10.1016/j.parint.2021.102358.

References

[1] World Health Organization, World Malaria Report 2019, World Health Organization, 2019. Geneva, Switzerland. ISBN: 978 92 4 156572 1.

[2] R.M. Fairhurst, A.M. Dondorp, Artemisinin-resistant *Plasmodium falciparum* malaria, Microbiol. Spectr. 4 (3) (2016), https://doi.org/10.1128/microbiolspec.EI10-0013-2016.

[3] T.F. de Koning-Ward, M.W. Dixon, L. Tilley, P.R. Gilson, *Plasmodium* species: master renovators of their host cells, Nat. Rev. Microbiol. 14 (8) (2016) 494–507, https://doi.org/10.1038/nrmicro.2016.79.

[4] M. Marti, R.T. Good, M. Rug, E. Knuepfer, A.F. Cowman, Targeting malaria virulence and remodeling proteins to the host erythrocyte, Science 306 (5703) (2004) 1930–1933, https://doi.org/10.1126/science.1102452.

[5] N.L. Hiller, S. Bhattacharjee, C. van Ooij, K. Liolios, T. Harrison, C. Lopez-Estraño, K. Haldar, A host-targeting signal in virulence proteins reveals a secretome in malarial infection, Science 306 (5703) (2004) 1934–1937, https://doi.org/10.1126/science.1102737.

[6] C. Grüring, A. Heiber, F. Kruse, S. Flemming, G. Franci, S.F. Colombo, E. Fasana, H. Schoeler, N. Borgese, H.G. Stunnenberg, J.M. Przyborski, T.W. Gilberger, T. Spielmann, Uncovering common principles in protein export of malaria parasites, Cell Host Microbe 12 (5) (2012) 717–729, https://doi.org/10.1016/j.chom.2012.09.010.

[7] A. Heiber, F. Kruse, C. Pick, C. Grüring, S. Flemming, A. Oberli, H. Schoeler, S. Retzlaff, P. Mesén-Ramírez, J.A. Hiss, M. Kadekoppala, L. Hecht, A.A. Holder, T. W. Gilberger, T. Spielmann, Identification of new PNEPs indicates a substantial non-PEXEL exportome and underpins common features in *Plasmodium falciparum* protein export, PLoS Pathog. 9 (8) (2013), e1003546, https://doi.org/10.1371/journal.ppat.1003546.

[8] B.M. Cooke, D.W. Buckingham, F.K. Glenister, K.M. Fernandez, L.H. Bannister, M. Marti, N. Mohandas, R.L. Coppel, A Maurer's cleft-associated protein is essential for expression of the major malaria virulence antigen on the surface of infected red blood cells, J. Cell Biol. 172 (6) (2006) 899–908, https://doi.org/10.1083/jcb.200509122.

[9] A.G. Maier, M. Rug, M.T. O'Neill, J.G. Beeson, M. Marti, J. Reeder, A.F. Cowman, Skeleton-binding protein 1 functions at the parasitophorous vacuole membrane to traffic PfEMP1 to the *Plasmodium falciparum*-infected erythrocyte surface, Blood 109 (3) (2007) 1289–1297, https://doi.org/10.1182/blood-2006-08-043364.

[10] A.G. Maier, M. Rug, M.T. O'Neill, M. Brown, S. Chakravorty, T. Szestak, J. Chesson, Y. Wu, K. Hughes, R.L. Coppel, C. Newbold, J.G. Beeson, A. Craig, B.S. Crabb, A. F. Cowman, Exported proteins required for virulence and rigidity of *Plasmodium falciparum*-infected human erythrocytes, Cell 134 (1) (2008) 48–61, https://doi.org/10.1016/j.cell.2008.04.051.

[11] R. Takano, H. Kozuka-Hata, D. Kondoh, H. Bochimoto, M. Oyama, K. Kato, A high-resolution map of SBP1 interactomes in *Plasmodium falciparum*-infected erythrocytes, iScience 19 (2019) 703–714, https://doi.org/10.1016/j.isci.2019.07.035.

[12] E. McHugh, O.M.S. Carmo, A. Blanch, O. Looker, B. Liu, S. Tiash, D. Andrew, S. Batinovic, A.J.Y. Low, H.J. Cho, P. McMillan, L. Tilley, M.W.A. Dixon, Role of *Plasmodium falciparum* protein GEXP07 in Maurer's cleft morphology, knob architecture, and *P. falciparum* EMP1 trafficking, mBio 11 (2) (2020), e03320-19, https://doi.org/10.1128/mBio.03320-19.

[13] J.A. Chan, F.J. Fowkes, J.G. Beeson, Surface antigens of *Plasmodium falciparum*-infected erythrocytes as immune targets and malaria vaccine candidates, Cell. Mol. Life Sci. 71 (19) (2014) 3633–3657, https://doi.org/10.1007/s00018-014-1614-3.

[14] N.D. Pasternak, R. Dzikowski, PfEMP1: an antigen that plays a key role in the pathogenicity and immune evasion of the malaria parasite *Plasmodium falciparum*, Int. J. Biochem. Cell Biol. 41 (7) (2009) 1463–1466, https://doi.org/10.1016/j.biocel.2008.12.012.

[15] S. Goel, M. Palmkvist, K. Moll, N. Joannin, P. Lara, R.R. Akhouri, N. Moradi, K. Öjemalm, M. Westman, D. Angeletti, H. Kjellin, J. Lehtiö, O. Blixt, L. Ideström, C.G. Gahmberg, J.R. Storry, A.K. Hult, M.L. Olsson, G. von Heijne, I. Nilsson, M. Wahlgren, RIFINs are adhesins implicated in severe *Plasmodium falciparum* malaria, Nat. Med. 21 (4) (2015) 314–317, https://doi.org/10.1038/nm.3812.

[16] M. Niang, A.K. Bei, K.G. Madnani, S. Pelly, S. Dankwa, U. Kanjee, K. Gunalan, A. Amaladoss, K.P. Yeo, N.S. Bob, B. Malleret, M.T. Duraisingh, P.R. Preiser, STEVOR is a *Plasmodium falciparum* erythrocyte binding protein that mediates merozoite invasion and rosetting, Cell Host Microbe 16 (1) (2014) 81–93, https://doi.org/10.1016/j.chom.2014.06.004.

[17] G. Winter, S. Kawai, M. Haeggström, O. Kaneko, A. von Euler, S. Kawazu, D. Palm, V. Fernandez, M. Wahlgren, SURFIN is a polymorphic antigen expressed on *Plasmodium falciparum* merozoites and infected erythrocytes, J. Exp. Med. 201 (11) (2005) 1853–1863, https://doi.org/10.1084/jem.20041392.

[18] T. Spielmann, T.W. Gilberger, Critical steps in protein export of *Plasmodium falciparum* blood stages, Trends Parasitol. 31 (10) (2015) 514–525, https://doi.org/10.1016/j.pt.2015.06.010.

[19] N. Gehde, C. Hinrichs, I. Montilla, S. Charpian, K. Lingelbach, J.M. Przyborski, Protein unfolding is an essential requirement for transport across the parasitophorous vacuolar membrane of *Plasmodium falciparum*, Mol. Microbiol. 71 (3) (2009) 613–628, https://doi.org/10.1111/j.1365-2958.2008.06552.x.

[20] K.M. Matthews, M. Kalanon, T.F. de Koning-Ward, Uncoupling the threading and unfoldase actions of *Plasmodium* HSP101 reveals differences in export between soluble and insoluble proteins, mBio 10 (3) (2019), e01106-19, https://doi.org/10.1128/mBio.01106-19.

[21] P. Mesén-Ramírez, F. Reinsch, A. Blancke Soares, B. Bergmann, A.K. Ullrich, S. Tenzer, T. Spielmann, Stable translocation intermediates jam global protein export in *Plasmodium falciparum* parasites and link the PTEX component EXP2 with translocation activity, PLoS Pathog. 12 (5) (2016), e1005618, https://doi.org/10.1371/journal.ppat.1005618.

[22] T.F. de Koning-Ward, P.R. Gilson, J.A. Boddey, M. Rug, B.J. Smith, A.T. Papenfuss, P.R. Sanders, R.J. Lundie, A.G. Maier, A.F. Cowman, B.S. Crabb, A newly discovered protein export machine in malaria parasites, Nature 459 (7249) (2009) 945–949, https://doi.org/10.1038/nature08104.

[23] H.E. Bullen, S.C. Charnaud, M. Kalanon, D.T. Riglar, C. Dekiwadia, N. Kangwanrangsan, M. Torii, T. Tsuboi, J. Baum, S.A. Ralph, A.F. Cowman, T.F. de Koning-Ward, B.S. Crabb, P.R. Gilson, Biosynthesis, localization, and macromolecular arrangement of the *Plasmodium falciparum* translocon of exported proteins (PTEX), J. Biol. Chem. 287 (11) (2012) 7871–7884, https://doi.org/10.1074/jbc.M111.328591.

[24] C.M. Ho, J.R. Beck, M. Lai, Y. Cui, D.E. Goldberg, P.F. Egea, Z.H. Zhou, Malaria parasite translocon structure and mechanism of effector export, Nature 561 (7721) (2018) 70–75, https://doi.org/10.1038/s41586-018-0469-4.

[25] J.R. Beck, V. Muralidharan, A. Oksman, D.E. Goldberg, PTEX component HSP101 mediates export of diverse malaria effectors into host erythrocytes, Nature 511 (7511) (2014) 592–595, https://doi.org/10.1038/nature13574.

[26] B. Elsworth, K. Matthews, C.Q. Nie, M. Kalanon, S.C. Charnaud, P.R. Sanders, S. A. Chisholm, N.A. Counihan, P.J. Shaw, P. Pino, J.A. Chan, M.F. Azevedo, S. J. Rogerson, J.G. Beeson, B.S. Crabb, P.R. Gilson, T.F. de Koning-Ward, PTEX is an essential nexus for protein export in malaria parasites, Nature 511 (7511) (2014) 587–591, https://doi.org/10.1038/nature13555.

[27] S.C. Charnaud, R. Kumarasingha, H.E. Bullen, B.S. Crabb, P.R. Gilson, Knockdown of the translocon protein EXP2 in *Plasmodium falciparum* reduces growth and protein export, PLoS One 13 (11) (2018), e0204785, https://doi.org/10.1371/journal.pone.0204785.

[28] M. Garten, A.S. Nasamu, J.C. Niles, J. Zimmerberg, D.E. Goldberg, J.R. Beck, EXP2 is a nutrient-permeable channel in the vacuolar membrane of *Plasmodium* and is essential for protein export via PTEX, Nat. Microbiol. 3 (10) (2018) 1090–1098, https://doi.org/10.1038/s41564-018-0222-7.

[29] K. Hakamada, H. Watanabe, R. Kawano, K. Noguchi, M. Yohda, Expression and characterization of the *Plasmodium* translocon of the exported proteins component EXP2, Biochem. Biophys. Res. Commun. 482 (4) (2017) 700–705, https://doi.org/10.1016/j.bbrc.2016.11.097.

[30] P.R. Sanders, B.K. Dickerman, S.C. Charnaud, P.A. Ramsland, B.S. Crabb, P. R. Gilson, The N-terminus of EXP2 forms the membrane-associated pore of the protein exporting translocon PTEX in *Plasmodium falciparum*, J. Biochem. 165 (3) (2019) 239–248, https://doi.org/10.1093/jb/mvy099.

[31] Q. Zhang, C. Ma, A. Oberli, A. Zinz, S. Engels, J.M. Przyborski, Proteomic analysis of exported chaperone/co-chaperone complexes of *P. falciparum* reveals an array of complex protein-protein interactions, Sci. Rep. 7 (2017) 42188, https://doi.org/10.1038/srep42188.

[32] S. Batinovic, E. McHugh, S.A. Chisholm, K. Matthews, B. Liu, L. Dumont, S. C. Charnaud, M.P. Schneider, P.R. Gilson, T.F. de Koning-Ward, M.W.A. Dixon, L. Tilley, An exported protein-interacting complex involved in the trafficking of virulence determinants in *Plasmodium*-infected erythrocytes, Nat. Commun. 8 (2017) 16044, https://doi.org/10.1038/ncomms16044.

[33] X. Zhu, K. Yahata, J.S. Alexandre, T. Tsuboi, O. Kaneko, The N-terminal segment of *Plasmodium falciparum* $SURFIN_{4.1}$ is required for its trafficking to the red blood cell cytosol through the endoplasmic reticulum, Parasitol. Int. 62 (2) (2013) 215–229, https://doi.org/10.1016/j.parint.2012.12.006.

[34] B.A. Chitama, S. Miyazaki, X. Zhu, W. Kagaya, K. Yahata, O. Kaneko, Multiple charged amino acids of *Plasmodium falciparum* $SURFIN_{4.1}$ N-terminal region are important for efficient export to the red blood cell, Parasitol. Int. 71 (2019) 186–193, https://doi.org/10.1016/j.parint.2019.04.019.

[35] C. Frech, N. Chen, Variant surface antigens of malaria parasites: functional and evolutionary insights from comparative gene family classification and analysis, BMC Genomics 14 (2013) 427, https://doi.org/10.1186/1471-2164-14-427.

[36] J.S. Alexandre, K. Yahata, S. Kawai, M. Torii, O. Kaneko, PEXEL-independent trafficking of *Plasmodium falciparum* $SURFIN_{4.2}$ to the parasite-infected red blood cell and Maurer's clefts, Parasitol. Int. 60 (3) (2011) 313–320, https://doi.org/10.1016/j.parint.2011.05.003.

[37] W. Kagaya, S. Miyazaki, K. Yahata, N. Ohta, O. Kaneko, The cytoplasmic region of *Plasmodium falciparum* $SURFIN_{4.2}$ is required for transport from Maurer's clefts to the red blood cell surface, Trop. Med. Health 43 (4) (2015) 265–272, https://doi.org/10.2149/tmh.2015-38.

[38] S. Haase, S. Herrmann, C. Grüring, A. Heiber, P.W. Jansen, C. Langer, M. Treeck, A. Cabrera, C. Bruns, N.S. Struck, M. Kono, K. Engelberg, U. Ruch, H. G. Stunnenberg, T.W. Gilberger, T. Spielmann, Sequence requirements for the export of the *Plasmodium falciparum* Maurer's clefts protein REX2, Mol. Microbiol. 71 (4) (2009) 1003–1017, https://doi.org/10.1111/j.1365-2958.2008.06582.x.

[39] S. Nakazawa, R. Culleton, Y. Maeno, *In vivo* and *in vitro* gametocyte production of *Plasmodium falciparum* isolates from Northern Thailand, Int. J. Parasitol. 41 (3–4) (2011) 317–323, https://doi.org/10.1016/j.ijpara.2010.10.003.

[40] D. Walliker, I.A. Quakyi, T.E. Wellems, T.F. McCutchan, A. Szarfman, W.T. London, L.M. Corcoran, T.R. Burkot, R. Carter, Genetic analysis of the human malaria parasite *Plasmodium falciparum*, Science 236 (4809) (1987) 1661–1666, https://doi.org/10.1126/science.3299700.

[41] L.J. Nkrumah, R.A. Muhle, P.A. Moura, P. Ghosh, G.F. Hatfull, W.R. Jacobs, D. A. Fidock, Efficient site-specific integration in *Plasmodium falciparum* chromosomes mediated by mycobacteriophage Bxb1 integrase, Nat. Methods 3 (8) (2006) 615–621, https://doi.org/10.1038/nmeth904.

[42] W. Trager, J.B. Jensen, Human malaria parasites in continuous culture, Science 193 (4254) (1976) 673–675, https://doi.org/10.1126/science.781840.

[43] K. Deitsch, C. Driskill, T. Wellems, Transformation of malaria parasites by the spontaneous uptake and expression of DNA from human erythrocytes, Nucleic Acids Res. 29 (3) (2001) 850–853, https://doi.org/10.1093/nar/29.3.850.

[44] K.J. Roux, D.I. Kim, M. Raida, B. Burke, A promiscuous biotin ligase fusion protein identifies proximal and interacting proteins in mammalian cells, J. Cell Biol. 196 (6) (2012) 801–810, https://doi.org/10.1083/jcb.201112098.
[45] G.G. van Dooren, M. Marti, C.J. Tonkin, L.M. Stimmler, A.F. Cowman, G. I. McFadden, Development of the endoplasmic reticulum, mitochondrion and apicoplast during the asexual life cycle of *Plasmodium falciparum*, Mol. Microbiol. 57 (2) (2005) 405–419, https://doi.org/10.1111/j.1365-2958.2005.04699.x.
[46] A.B. Lucky, M. Sakaguchi, Y. Katakai, S. Kawai, K. Yahata, T.J. Templeton, O. Kaneko, *Plasmodium knowlesi* skeleton-binding protein 1 localizes to the 'Sinton and Mulligan' stipplings in the cytoplasm of monkey and human erythrocytes, PLoS One 11 (10) (2016), e0164272, https://doi.org/10.1371/journal.pone.0164272.
[47] S. Kikuchi, M. Oishi, Y. Hirabayashi, D.W. Lee, I. Hwang, M. Nakai, A 1-megadalton translocation complex containing Tic20 and Tic21 mediates chloroplast protein import at the inner envelope membrane, Plant Cell 21 (6) (2009) 1781–1797, https://doi.org/10.1105/tpc.108.063552.
[48] T. Tsuboi, S. Takeo, H. Iriko, L. Jin, M. Tsuchimochi, S. Matsuda, E.T. Han, H. Otsuki, O. Kaneko, J. Sattabongkot, R. Udomsangpetch, T. Sawasaki, M. Torii, Y. Endo, Wheat germ cell-free system-based production of malaria proteins for discovery of novel vaccine candidates, Infect. Immun. 76 (4) (2008) 1702–1708, https://doi.org/10.1128/IAI.01539-07.
[49] K. Marumo, K. Nakada-Tsukui, K. Tomii, T. Nozaki, Ligand heterogeneity of the cysteine protease binding protein family in the parasitic protist *Entamoeba histolytica*, Int. J. Parasitol. 44 (9) (2014) 625–635, https://doi.org/10.1016/j.ijpara.2014.04.008.
[50] D. Ito, E.T. Han, S. Takeo, A. Thongkukiatkul, H. Otsuki, M. Torii, T. Tsuboi, *Plasmodial* ortholog of *Toxoplasma gondii* rhoptry neck protein 3 is localized to the rhoptry body, Parasitol. Int. 60 (2) (2011) 132–138, https://doi.org/10.1016/j.parint.2011.01.001.
[51] J. Cao, O. Kaneko, A. Thongkukiatkul, M. Tachibana, H. Otsuki, Q. Gao, T. Tsuboi, M. Torii, Rhoptry neck protein RON2 forms a complex with microneme protein AMA1 in *Plasmodium falciparum* merozoites, Parasitol. Int. 58 (1) (2009) 29–35, https://doi.org/10.1016/j.parint.2008.09.005.
[52] B. Elsworth, P.R. Sanders, T. Nebl, S. Batinovic, M. Kalanon, C.Q. Nie, S. C. Charnaud, H.E. Bullen, T.F. de Koning Ward, L. Tilley, B.S. Crabb, P.R. Gilson, Proteomic analysis reveals novel proteins associated with the *Plasmodium* protein exporter PTEX and a loss of complex stability upon truncation of the core PTEX component, PTEX150, Cell. Microbiol. 18 (11) (2016) 1551–1569, https://doi.org/10.1111/cmi.12596.
[53] D. Ito, M.A. Schureck, S.A. Desai, An essential dual-function complex mediates erythrocyte invasion and channel-mediated nutrient uptake in malaria parasites, Elife 6 (2017), e23485, https://doi.org/10.7554/eLife.23485.
[54] L.M. Low, Y. Azasi, E.S. Sherling, M. Garten, J. Zimmerberg, T. Tsuboi, J. Brzostowski, J. Mu, M.J. Blackman, L.H. Miller, Deletion of *Plasmodium falciparum* protein RON3 affects the functional translocation of exported proteins and glucose uptake, mBio 10 (4) (2019), e01460-19, https://doi.org/10.1128/mBio.01460-19.
[55] P.R. Sanders, P.R. Gilson, G.T. Cantin, D.C. Greenbaum, T. Nebl, D.J. Carucci, M. J. McConville, L. Schofield, A.N. Hodder, J.R. Yates, B.S. Crabb, Distinct protein classes including novel merozoite surface antigens in raft-like membranes of *Plasmodium falciparum*, J. Biol. Chem. 280 (48) (2005) 40169–40176, https://doi.org/10.1074/jbc.M509631200.
[56] P.R. Sanders, G.T. Cantin, D.C. Greenbaum, P.R. Gilson, T. Nebl, R.L. Moritz, J. R. Yates, A.N. Hodder, B.S. Crabb, Identification of protein complexes in detergent-resistant membranes of *Plasmodium falciparum* schizonts, Mol. Biochem. Parasitol. 154 (2) (2007) 148–157, https://doi.org/10.1016/j.molbiopara.2007.04.013.
[57] X.Y. Yam, C. Birago, F. Fratini, F. Di Girolamo, C. Raggi, M. Sargiacomo, A. Bachi, L. Berry, G. Fall, C. Currà, E. Pizzi, C.B. Breton, M. Ponzi, Proteomic analysis of detergent-resistant membrane microdomains in trophozoite blood stage of the human malaria parasite *Plasmodium falciparum*, Mol. Cell. Proteomics 12 (12) (2013) 3948–3961, https://doi.org/10.1074/mcp.M113.029272.
[58] D.T. Riglar, K.L. Rogers, E. Hanssen, L. Turnbull, H.E. Bullen, S.C. Charnaud, J. Przyborski, P.R. Gilson, C.B. Whitchurch, B.S. Crabb, J. Baum, A.F. Cowman, Spatial association with PTEX complexes defines regions for effector export into *Plasmodium falciparum*-infected erythrocytes, Nat. Commun. 4 (2013) 1415, https://doi.org/10.1038/ncomms2449.
[59] M. Morita, H. Nagaoka, E.H. Ntege, B.N. Kanoi, D. Ito, T. Nakata, J.W. Lee, K. Tokunaga, T. Iimura, M. Torii, T. Tsuboi, E. Takashima, PV1, a novel *Plasmodium falciparum* merozoite dense granule protein, interacts with exported protein in infected erythrocytes, Sci. Rep. 8 (1) (2018) 3696, https://doi.org/10.1038/s41598-018-22026-0.
[60] T. Spielmann, D.L. Gardiner, H.P. Beck, K.R. Trenholme, D.J. Kemp, Organization of ETRAMPs and EXP-1 at the parasite-host cell interface of malaria parasites, Mol. Microbiol. 59 (3) (2006) 779–794, https://doi.org/10.1111/j.1365-2958.2005.04983.x.
[61] F. Galaway, L.G. Drought, M. Fala, N. Cross, A.C. Kemp, J.C. Rayner, G.J. Wright, P113 is a merozoite surface protein that binds the N terminus of *Plasmodium falciparum* RH5, Nat. Commun. 8 (2017) 14333, https://doi.org/10.1038/ncomms14333.
[62] V. Offeddu, M. Rauch, O. Silvie, K. Matuschewski, The *Plasmodium* protein P113 supports efficient sporozoite to liver stage conversion *in vivo*, Mol. Biochem. Parasitol. 193 (2) (2014) 101–109, https://doi.org/10.1016/j.molbiopara.2014.03.002.
[63] M. Zhang, C. Wang, T.D. Otto, J. Oberstaller, X. Liao, S.R. Adapa, K. Udenze, I. F. Bronner, D. Casandra, M. Mayho, J. Brown, S. Li, J. Swanson, J.C. Rayner, R.H. Y. Jiang, J.H. Adams, Uncovering the essential genes of the human malaria parasite *Plasmodium falciparum* by saturation mutagenesis, Science 360 (6388) (2018), https://doi.org/10.1126/science.aap7847 eaap7847.
[64] E. Lasonder, S.R. Rijpma, B.C. van Schaijk, W.A. Hoeijmakers, P.R. Kensche, M. S. Gresnigt, A. Italiaander, M.W. Vos, R. Woestenenk, T. Bousema, G.R. Mair, S. M. Khan, C.J. Janse, R. Bártfai, R.W. Sauerwein, Integrated transcriptomic and proteomic analyses of *P. falciparum* gametocytes: molecular insight into sex-specific processes and translational repression, Nucleic Acids Res. 44 (13) (2016) 6087–6101, https://doi.org/10.1093/nar/gkw536.
[65] G. Zanghì, S.S. Vembar, S. Baumgarten, S. Ding, J. Guizetti, J.M. Bryant, D. Mattei, A.T.R. Jensen, L. Rénia, Y.S. Goh, R. Sauerwein, C.C. Hermsen, J.F. Franetich, M. Bordessoulles, O. Silvie, V. Soulard, O. Scatton, P. Chen, S. Mecheri, D. Mazier, A. Scherf, A specific PfEMP1 is expressed in *P. falciparum* sporozoites and plays a role in hepatocyte infection, Cell Rep. 22 (11) (2018) 2951–2963, https://doi.org/10.1016/j.celrep.2018.02.075.
[66] S. Kenthirapalan, A.P. Waters, K. Matuschewski, T.W. Kooij, Functional profiles of orphan membrane transporters in the life cycle of the malaria parasite. Nat. Commun. 7 (2016), 10519 https://doi.org/10.1038/ncomms10519.